The Astronomical Journal, 127:1029–1051, 2004 February

STELLAR ROTATION IN YOUNG CLUSTERS: THE FIRST 4 MILLION YEARS

L. M. Rebull,[1,2] S. C. Wolff,[3] and S. E. Strom[3]

Received 2003 June 3; accepted 2003 October 16

ABSTRACT

To investigate what happens to angular momentum during the earliest observable phases of stellar evolution, we searched the literature for periods (P), projected rotational velocities ($v \sin i$), and supporting data on K5–M2 stars (corresponding to masses 0.25–1 $M_{\odot}$) from the Orion Nebula Cluster and environs, ρ Ophiuchi, TW Hydra, Taurus-Auriga, NGC 2264, Chamaeleon, Lupus, and η Chamaeleonis. We combine these measures of rotation with the stellar R (as determined from $L_{\rm bol}$ and $T_{\rm eff}$) to compare the data with two extreme cases: conservation of stellar angular velocity and conservation of stellar angular momentum. Analysis of the P data set suggests that the frequency distribution of periods among the youngest and oldest stars in the sample is indistinguishable, while the $v \sin i$ data set reveals a decrease in mean $v \sin i$ as a function of age. Both results suggest that a significant fraction of all pre–main-sequence (PMS) stars must evolve at nearly constant angular velocity during the first $\sim$3–5 Myr after they begin their evolution down the convective tracks. Hence, the angular momenta of a significant fraction of pre–main-sequence (PMS) stars must be tightly regulated during the first few million years after they first become observable. This result seems surprising at first glance, because observations of young main-sequence stars reveal a population (30%–40%) of rapidly rotating stars that must begin to spin up at ages $t \ll 5$ Myr. To determine whether these apparently contradictory results are reconcilable, we use simple models along with our data set to place limits on (1) the fraction of PMS stars that must be regulated, and (2) the complementary fraction that could spin up as a function of time but escape statistical detection given the broad distribution of stellar rotation rates. These models include (1) instantaneous release at the stellar birthline of a given fraction of stars, with the remaining fraction regulated for 10 Myr; (2) all stars regulated initially, with the released fraction varying linearly with time, and timescales for release of half the stars varying from 0.5 to 5 Myr (i.e., all released by 1 to 10 Myr); and (3) a hybrid model that invokes assumptions (1) and (2). In all cases, we find that a modest population (30%–40%) of PMS stars could be released within the first 1 Myr and still produce period distributions statistically consistent with the observed data. This population is large enough to account for the rapid rotators observed among young main-sequence stars of comparable mass. The limits placed by our models on the fraction of regulated and released stars as a function of time are also consistent with the lifetime of accretion disks as inferred from near-IR excesses, and hence with the hypothesis that disk locking accounts for rotation regulation during early PMS phases.

Key words: stars: rotation

On-line material: machine-readable table

1. INTRODUCTION

Over the past decade, theory and observation have produced a standard model of star formation in which pre–main-sequence (PMS) stars accumulate a substantial portion of their final mass through rapid accretion ($\sim 10^{-5}\ M_{\odot}\ {\rm yr}^{-1}$) of material transported through circumstellar disks. When this rapid accretion phase ends, stars are deposited on the birthline (e.g., Stahler 1983). Accretion may continue at a lower rate ($\sim 10^{-8}\ M_{\odot}\ {\rm year}^{-1}$) while stars evolve down their convective tracks.

Models attempt to account for the rotation rates of the main-sequence descendants of PMS stars by evolving the observed distribution of rotation rates in star-forming regions forward in time. These models must account for (1) a large population of slow rotators that require significant stellar angular momentum loss sometime during the course of evolution from the birthline to the zero-age main sequence (ZAMS); and (2) a smaller population of rapid rotators that require conservation of stellar angular momentum, resulting in significant spin-up as stars contract along convective tracks from the birthline to the ZAMS (e.g., Bouvier et al. 1997b; Bouvier, Forestini, & Allain 1997a; Tinker, Pinsonneault, & Terndrup 2002 and references therein). Mechanisms proposed to account for the angular momentum loss of fully convective PMS stars typically invoke angular momentum transfer either from the star to the surrounding accretion disk (e.g., Königl 1991, Königl & Pudritz 2000) or to a stellar wind originating at the boundary between the disk and the stellar magnetosphere (e.g., Shu et al. 2000). Either mechanism predicts that, during the disk-accretion phase, the angular velocity of the star should be approximately "locked" to a period set by the Keplerian angular velocity at or near the boundary between the stellar magnetosphere and the accretion disk. At the end of the accretion phase, PMS stars should be unlocked from their disks and free to spin up as they contract toward the main sequence. (See Mathieu 2003 for a recent review of observations.)

In this paper, we examine what happens to stellar angular momentum during the first 3–5 Myr after stars are deposited on their birthlines. To do so, we searched the literature for

[1] *Spitzer* Science Center, California Institute of Technology, Mail Stop 220-6, 1200 East California Boulevard, Pasadena, CA 91125; luisa.rebull@jpl.nasa.gov.

[2] Some of this work was carried out as a National Research Council Resident Research Associate, Jet Propulsion Laboratory, California Institute of Technology, 4800 Oak Grove Drive, Pasadena, CA 91109.

[3] National Optical Astronomical Observatory, 950 North Cherry Avenue, Tucson, AZ 85726.

periods (P) and projected rotational velocities ($v \sin i$) for K5–M2 stars in eight clusters that contain PMS stars on convective tracks. We use these observations to constrain the fraction of stars that must be regulated as a function of time during PMS phases rather than attempting to test specific models.

This age range is particularly sensitive to changes in stellar angular momentum from the rapid changes in stellar radius that characterize early evolutionary stages of low-mass PMS stars. For a star of mass $\sim 0.5\ M_{\odot}$, the radius changes by a factor of ~ 3 between the birthline and an age of 3 Myr; beyond 3 Myr, the radius changes by a factor of less than 1.5. This rapid change in radius during the first 3–5 Myr can lead to rapid divergence in rotational velocity or period between (1) stars whose angular velocity is regulated by some extrinsic mechanism (as above) and is not allowed to change as the star evolves during the first ~ 3–5 Myr; and (2) stars that are free to spin up as they contract. In turn, this should, in principle, enable us to determine the fraction of stars that are regulated and released as a function of time. Specifically, if angular velocity (Ω) is constant as stars evolve, then

$$\Omega \propto v/R = \text{constant}, \tag{1}$$

meaning that v varies directly with R and the period P remains constant. If instead angular momentum (J) is conserved, then

$$J = I\omega \propto MvR = \text{constant}, \tag{2}$$

where we have assumed that the star can be approximated by a sphere for which $I \propto MR^2$. For fully convective PMS stars in the spectral type range K5–M2, stellar models show that this scaling approximation holds from the birthline to the ZAMS (see, e.g., Swenson et al. 1994). In this case, vR is constant and P varies as R^2. Given these relationships, the most direct way to search for changes in angular momentum with time is to look for correlations of P and $v \sin i$ with R.

For those stars for which angular velocity is conserved, we expect v to decrease by about a factor of 3 as the radius decreases by a factor of 3, while P remains constant. If angular momentum is conserved, we expect v to increase by a factor of 3, while P decreases by a factor of 9. For a typical initial velocity of 30 km s^{-1} near the top of the convective track, the velocity expected for our oldest stars is 10 km s^{-1} if angular velocity is conserved and 90 km s^{-1} if angular momentum is conserved. For a typical period of 5 days at the top of the convective track, we expect a period of 0.6 days at $t \sim 3$ Myr if angular momentum is conserved, but the same period of 5 days if angular velocity is conserved.

A previous search aimed at detecting evolutionary trends in stellar periods by Rebull et al. (2002a, hereafter RWSM02) was limited to stars in NGC 2264, the Orion Flanking Fields, and the Orion Nebula Cluster (ONC). The advantage of limiting that study to those three regions was that the completeness of the surveys with respect to P and $v \sin i$ was well understood. There were, however, several limitations of this earlier study. First, we included $v \sin i$ data only for stars in the ONC, a region where errors in the derived values of R are likely to be large because of large and anomalous reddening within the ONC region, and where high disk accretion rates affect the spectral energy distributions and hence the colors of accreting PMS stars of a given spectral type. By extending the study to older regions with lower reddening, we can reduce these two effects and also double the sample size, thereby adding statistical weight to the results, particularly for older PMS stars. Furthermore, our earlier study included only a few stars for which measurements of both P and $v \sin i$ are available. For the larger sample discussed below, there are many more stars for which both quantities are available, thus enabling an independent check on the accuracy of the measurements of R. By adding data from a larger sample of clusters, we can also obtain a number of stars sufficient to restrict the objects under consideration to a narrow mass range (K5–M2) in which the errors in R are smaller than for stars with earlier or later spectral types (see RWSM02). This comprehensive inventory of extant data in young clusters can also serve to guide future rotation surveys.

Accordingly, in order to obtain the largest sample currently possible, we have searched the literature for all of the available data on either P or $v \sin i$ for PMS stars in eight young clusters. In order to derive stellar radii, we also require that both spectral types and colors have been measured. We then use these data to explore the following issues:

1. For those stars for which both P and $v \sin i$ have been measured, does R as derived from $L_{\rm bol}$ and $T_{\rm eff}$ correlate well with $R \sin i$ derived from P and $v \sin i$? In other words, can we determine R with sufficient accuracy to search for statistically significant correlations between P and $v \sin i$ with R?
2. Do we see systematic changes in either P or $v \sin i$ with R, which, in effect, constrain how angular momentum changes as stars contract?
3. Can this more extensive data set be used to put limits on when stars begin to spin up? Are these estimates consistent with independent estimates of rotation regulation and with the rotation rates of the young main-sequence descendants of PMS stars?

In § 2, we discuss the data we extracted from the literature and the initial analysis steps. In § 3, we proceed with the main analysis, deriving the evolution of $v \sin i$ and P as a function of R, and discuss the implications of our findings. We conclude in § 4.

2. DATA AND BASIC ANALYSIS

In this section, we review the data we used for this analysis (§ 2.1), the method for calculating stellar R (§ 2.2), and the completeness and biases of these data (§ 2.3).

2.1. *Cluster Data*

We searched the literature for rotation and supporting data on young stars. There are only eight young clusters where there are appreciable numbers of stars with V and I magnitudes, spectral types, and rotational information (P or $v \sin i$). These clusters are the Orion Nebula Cluster and environs, NGC 2264, Taurus-Auriga, ρ Ophiuchi, TW Hydra, Chamaeleon, Lupus, and η Chamaeleonis. We also compiled data for young clusters in which low-mass stars have already reached the zero-age main sequence (ZAMS): IC 2391 & IC 2602, α Persei, and the Pleiades. A data table and a description of the data (and references) for each individual cluster is included in the Appendix.

Table 1 lists the number of members with some rotation information (either P or $v \sin i$ or both) for each of the clusters in our survey. We limit the analysis that follows to those stars with spectral types in the range K5–M2. The lower mass limit was set at M2, because stars with later spectral types have progressively larger errors in R (see below and RWSM02). The upper mass limit was chosen because stars later than K5

TABLE 1
NUMBER OF AVAILABLE STARS (WITH SPECTRAL TYPE, V, I, AND SOME ROTATIONAL INFORMATION)

Cluster	Total	No. with P	No. with $v \sin i$	No. with Both P and $v \sin i$	Total K5–M2	No. with P (K5–M2)	No. with $v \sin i$ (K5–M2)	No. with Both P and $v \sin i$[a]
Orion	623	480	286	143	234	206	101	73
Cham	40	10	39	9	18	5	17	4
ρ Oph	9	5	5	1	5	2	4	1
NGC 2264.....	188	144	61	17	102	92	18	8
Tau-Aur	123	61	122	60	65	38	65	38
Lupus.....	76	40	69	33	37	21	32	16
η Cha.....	12	12	0	0	5	5	0	0
TW Hya	36	1	36	1	19	1	19	1
IC 2391/2602	51	27	46	22	9	7	5	3
α Per.....	87	41	81	35	25	16	19	10
Pleiades	140	43	136	39	45	13	41	9

[a] Includes upper limits for $v \sin i$. Omitting the upper limits in this column leaves 43 stars in Orion, 7 stars in NGC 2264, 32 stars in Tau-Aur, 15 stars in Lupus, 3 stars in Cham, none in TW Hya, and 2 stars in IC 2391/2602.

stay in (or at least close to) this spectral type range as they age because of the shape of their evolutionary tracks. Stars that begin life as early K stars will wind up as late G stars on the main sequence.

Table 2 lists the basic data for each of the clusters included in the current study. References can be found in the Appendix. The second column lists the range of ages of the stars in the cluster as estimated from the models by D'Antona & Mazzitelli (1994; hereafter DAM) and the values of R that we derived (see § 2.2 below). The third column gives the range of ages estimated in the literature. The remaining columns give the extinction in I_C, the distance modulus, the distance in parsecs along with an estimated uncertainty, the angular size or depth of the cluster along the line of sight, and the cluster density. An independent check on the consistency of these distance estimates is given in § 3.1.

2.2. *Calculation of R*

Regardless of what values of R, mass, or age might have been reported for an individual star in the literature, we calculated these quantities again to make the ensemble internally consistent. As in RWSM02, R for each star in the current sample was calculated from L_{bol} and T_{eff}

$$R^2 = L_{bol}/4\pi\sigma T_{eff}^4. \quad (3)$$

To obtain L_{bol} and T_{eff} from the observed I_C and $(V-I_C)$, we first dereddened the observed $(V-I_C)$, using the observed spectral type to estimate intrinsic colors; T_{eff} follows from the spectral type. The dereddened $I_{C,0}$ is calculated from the extinction at I_C, which is given by $A_I = 1.61E\ (V-I_C)$. We convert $I_{C,0}$ to L_{bol}, using the approach described by Hillenbrand (1997); distance moduli were taken from the literature as noted in the Appendix. Our photospheric colors for each spectral type include measurements from Bessell (1991), Leggett (1992), and Leggett et al. (1998). The most likely A_I in Table 2 was used only if the measured $(V-I_C)$ was too blue for the expected photospheric color. In those (rare) cases, as in Rebull et al. (2000) and Rebull et al. (2002b), we did not deredden the $(V-I_C)$ color but corrected the V and I_C magnitudes separately by the most likely reddening in Table 2, thereby dereddening the L_{bol} estimate.

Masses for stars can be estimated from the dereddened color-magnitude diagram (CMD), combined with a set of models as in Rebull et al. (2000). If we use model 1 from DAM, the masses of the stars in our sample fall in the range 0.3–1 $M_\odot$; 90% of the sample falls between 0.3 and 0.8 $M_\odot$.

Key to the detection of systematic changes in P or v with R is the ability to estimate stellar radii with an accuracy that is a small fraction of the total change in R. An extensive discussion of the potential sources of errors in R has been given by RWSM02. The main conclusions of that discussion were that the errors were smallest for spectral types K5–M2, that typical errors in $\log R$ in this spectral range were $\sim$0.05 dex, and that a reasonable upper limit to the error was $\sim$0.13 dex. Similar analyses by Hartigan, Strom, & Strom (1994) and by Hartmann (2001) estimated the errors in R to be in the range 0.05–0.1 dex, with the larger errors applying to stars with high accretion rates, which may affect the colors and magnitudes, and to members of clusters that are extended along the line of sight. An independent confirmation of these error estimates is given in § 3.1, and they are sufficient for our analysis.

The estimated errors in R from the estimated error in the distance and from the estimated depth of the cluster along the line of sight for stars with types K5–M2 are listed explicitly for each cluster in Table 3.

2.3. *Sensitivity, Completeness, and Biases*

In this study, we are combining data from more than 100 published studies. Consequently, the final database is extremely inhomogeneous, and it is impossible to quantify the biases, strengths, limitations, and completeness of all the individual data sets. (However, certain clusters stand out as having better or worse coverage; see cluster discussions in Appendix.) One advantage of making use of both P and $v \sin i$ measurements is that the intrinsic biases for the two data sets are very different. Any reinforcing correlations found in both sets of data are unlikely to be solely the result of selection effects.

An advantage of the spectroscopic studies is that $v \sin i$ can be measured for any star for which a spectrum of adequate signal-to-noise can be obtained. The primary bias in spectroscopic determinations of $v \sin i$ results from the fact that most observations only have sufficient resolution to measure velocities >11 km s^{-1} (corresponding to $P < 6$ days) for a typical PMS star in the spectral range K5–M2. Hence, slowly rotating stars have only upper limits.

TABLE 2
CLUSTER AGES, REDDENING, DISTANCES, AND DENSITIES

Cluster	DAM Age Range from Data (Myr)	Age in Literature (Myr)	A_I[a]	$m-M$	Distance (pc)	Angular Size or Depth	Density (stars pc^{-3})
Orion	0.1–10	1–3	0.25[b]	8.36	470 ± 70	$\sim1^\circ$	10^4
Cham	0.3–4	1–20	0.92	6.02	160 ± 20	$\sim3^\circ$	~2–3
ρ Oph	~1	0.1–3	clumpy	5.57	130 ± 15	$\sim1^\circ$	10^4
NGC 2264	0.3–10	3–5	0.25	9.40	760 ± 30	$\sim1^\circ$	~1–2
Tau-Aur	1–10	1–10	0.37	5.73	140 ± 10	$\sim$20 pc	~1–10
Lupus	0.3–10	1–7	~0	5.88	150 ± 30	$\sim15^\circ$	~2
η Cha	3	4–9	~0	4.93	97 ± 4	$\sim2^\circ$	~1–2
TW Hya	~10	10	~0	3.89	60 ± 30	~10–12°	$\lesssim1$
IC 2391/2602	~10	30–50	0.027	5.95	155 ± 5	$\sim$10 pc	~1–3
α Per	>10	50–90	0.17	6.23	175 ± 10	$\sim$10 pc	~1
Pleiades	>30	115	0.07	5.60	132 ± 15	13 pc	$\lesssim1$

[a] Values of A_I are tabulated here to give a general indication of the interstellar reddening toward each cluster; all stars used in this analysis had spectral types and therefore derived A_I values specific to each star; see text.
[b] $A_I = 0.25$ in Flanking Fields, regions that surround but do not include Trapezium; see Rebull et al. 2000 and Rebull 2001. In the Trapezium region, the reddening is more clumpy.

Although periods can be obtained to very high precision, not all known PMS stars vary periodically. Aside from the fact that stars with strong accretion signatures seem less likely to vary periodically (Rebull 2001; Herbst, Bailer-Jones, & Mundt 2001), it is unclear what determines whether or not a star will show detectable periodic brightness variations. However, a recent study of likely PMS member stars in the ONC (Rhode, Herbst, & Mathieu 2001) indicates that there is no statistically significant difference between the $v \sin i$ distributions of the periodic stars and stars in a control sample for which periods are not known. This result suggests an ensemble of periodic variables provides a representative sample of the rotational properties of young stars.

3. ANALYSIS

In § 3.1, we compare R and $R \sin i$ to estimate the errors in our calculation of R and the relative distances we used for these clusters. Then in § 3.2, we consider the evolution of $v \sin i$ and P with R for the eight young clusters in our sample. We construct some simple models to test what might be hidden in the scatter in the data in § 3.3. In § 3.4, we compare the results for the young clusters with four older clusters and determine when stars must spin up in order to account for rotation rates in the older clusters. We compare our regulation timescales to disk lifetimes in § 3.5 and consider the feasibility of distinguishing rotation rates of disked and nondisked stars in § 3.6.

3.1. R *versus* $R \sin i$

In this section, we show that the claim that $\log R$ can be calculated to an accuracy of about 15% of the observed range is valid for the current data set. This is sufficient to detect systematic trends, if any, in the rotation rate as stars contract.

We have two independent methods of estimating the radii. First, we can calculate R from $T_{\rm eff}$ and $L_{\rm bol}$ as outlined in § 2. Second, if both P and $v \sin i$ have been measured, then we can find $R \sin i$ from

$$R \sin i = (v \sin i) P / 2\pi. \quad (4)$$

The comparison of R and $R \sin i$ for the 96 stars in our sample with both measured P and $v \sin i$ is shown in Figure 1. (We excluded five stars for which $\sin i$ as derived from the comparison of R and $R \sin i$ was larger than 1.5, on the

TABLE 3
ERRORS IN $\log R$ FROM DISTANCE AND WIDTH

Cluster	Error Due to Distance Error[a]	Error Due to Width[b]	Net Error[c]
Orion	0.06	0.01	0.06
Cham	0.05	0.02	0.05
ρ Oph	0.05	0.01	0.05
NGC 2264	0.02	0.01	0.02
Tau-Aur	0.03	0.05	0.06
Lupus	0.08	0.11	0.14
η Cha	0.01	0.01	0.01
TW Hya	0.17	0.07	0.18
IC 2391/2602	0.02	0.03	0.04
α Per	0.02	0.02	0.03
Pleiades	0.05	0.04	0.06

[a] Systematic error due to uncertainty in distance to cluster quoted in Table 2 above.
[b] Systematic error due to width of cluster along the line of sight, quoted in Table 2 above.
[c] Errors due to uncertainty in distance and width added in quadrature.

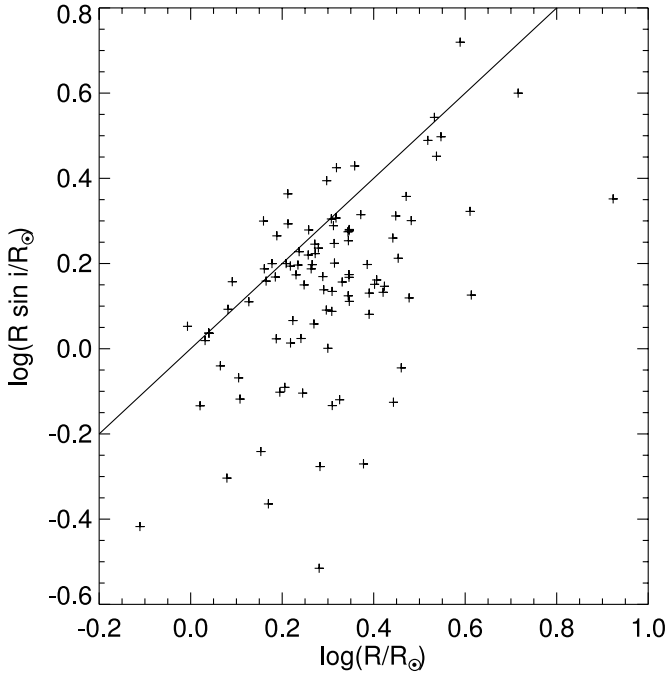

FIG. 1.—Plot of $\log R$ and $\log (R \sin i)$ for the 96 K5–M2 stars in our sample with both P and $v \sin i$ measured (no upper limits). We dropped five stars for which $\sin i > 1.5$. The line is the ideal case of $R = R \sin i$. Most of the scatter here comes from uncertainties in $\sin i$; when that is accounted for, this plot validates the claim that $\log R$ can be calculated with an accuracy of $\sim$0.08 dex.

assumption that the measurement of either $v \sin i$ or P was significantly in error, i.e., that those errors dominate over those from calculation of R.)

At first glance, the scatter in Figure 1 appears quite large. However, most of this scatter is expected, because of variations in $\sin i$, and is, in fact, consistent with what is expected from variations in i. For example, if i is distributed randomly, then we would expect to measure $v \sin i$ to be less than half of its true value only 15% of the time. In Figure 1, 16% ($\pm$4% by Poisson statistics) of the values lie more than a factor of 2 below the line. If both R and $R \sin i$ were known perfectly and if we had a large sample of points for which i is distributed randomly, then the standard deviation of a single measurement of $\log(R \sin i)$ from the true value of $\log R$ would be expected to be 0.22. By comparison, the mean error by which points in Figure 1 fall below the 45° straight line is 0.24, within 0.02 dex of the expected value.

If we now make the assumptions that the uncertainties in $\log(R \sin i)$, $\log R$, and $\sin i$ add in quadrature and that the standard errors in $\log(\sin i)$ and in the measured value of $v \sin i$ are 0.22 and 10% respectively, then we estimate the formal error in $\log R$ to be 0.08 dex. This is consistent with the error estimates of 0.05–0.10 dex cited earlier. We thus conclude that the R values estimated from $L_{\rm bol}$ and $T_{\rm eff}$ are sufficient to detect systematic trends in rotation rate.

In plotting Figure 1, we combined data for all of the K5–M2 stars in all of the young clusters for which both P and $v \sin i$ have been measured. If the relative distances of the clusters were significantly in error, this procedure would introduce scatter. In order to check for errors in distance, we determined the average value of $\sin i$ for each cluster for which we have sufficient data. Since $\sin i$ is given by

$$\sin i \propto (v \sin i) P T_{\rm eff}^2 L^{-1/2}, \quad (5)$$

errors in distance will result in systematic differences in the calculated value of the mean $\sin i$ ($\langle \sin i \rangle$) for the different clusters. The values of $\langle \sin i \rangle$ calculated for the data in Figure 1, again including only those stars for which formal values of $\sin i < 1.5$ and only those clusters with >5 points, are given in Table 4. The total range in $\log \langle \sin i \rangle$ is 0.07. This difference does not have a strong impact on the scatter in Figure 1. Since $\langle \sin i \rangle$ depends directly on the distance, this agreement suggests that the distances to at least the four most data-rich clusters are consistent to about 10%.

The expected value for $\langle \sin i \rangle$ for a random distribution of axes is 0.79. For the entire sample of stars, we find $\langle \sin i \rangle = 0.83$. If we exclude the five stars with formal values of $\sin i > 1.5$, we find 0.76. Table 4 collects the values of $\langle \sin i \rangle$ for each cluster separately. A low value of $\sin i$ for Orion was also found by Rhode et al. (2001), who discussed a number of potential explanations, including the possibility that the assigned temperatures were too low by 400–600 K. The fact that we find a value closer to what is expected for the entire sample suggests that a gross miscalibration of the atmospheric parameters may not be the explanation. We do note, however, that the distribution of i for the current sample contains too many stars with intermediate inclination angles (40°–60°) and too few with larger inclinations relative to what is expected for a random distribution of axes. An exploration of this discrepancy is outside the scope of the present paper. If the explanation is some kind of miscalibration that affects all of the stars, then we can still order the stars accurately according to their relative radii, even though the absolute values may be systematically in error. Alternatively, models suggest that the preferred latitude of appearance of the spots needed to measure P depends on both age and rotation rate (Granzer et al. 2000). If these models are correct, then we would tend to view more rapidly rotating and younger stars at smaller values of i, thereby skewing the distribution of i but not affecting the derived values of R.

In summary, although there are several sources of error that might affect the derivation of R, the dominant sources of error in the spectral range K5–M2 remain those described in RWSM02, and the good correlation between R and $R \sin i$ shows that R can be determined with sufficient accuracy to search for trends in P and $v \sin i$ with R, particularly since we have hundreds of stars with which to establish such correlations.

3.2. *Evolution of $v \sin i$ and P*

The availability of data for both $v \sin i$ and P for a large sample of stars over a large range in R provides a strong test of how angular momentum changes with time for typical PMS stars over the age range $t < 5$ Myr. Specifically, our data span $\log R \sim 0.6-0.1$ (a range of a factor of 3), which

TABLE 4

$\langle \sin i \rangle$ FOR YOUNG CLUSTERS WITH MORE THAN FIVE STARS AVAILABLE

Cluster	No. of Stars	$\langle \sin i \rangle$[a]
Orion	43	0.69 ± 0.04
Tau-Aur	32	0.82 ± 0.04
Lupus	15	0.72 ± 0.07
NGC 2264	7	0.85 ± 0.12
All data	96	0.76 ± 0.28

[a] Outliers with $\sin i > 1.5$ have been omitted.

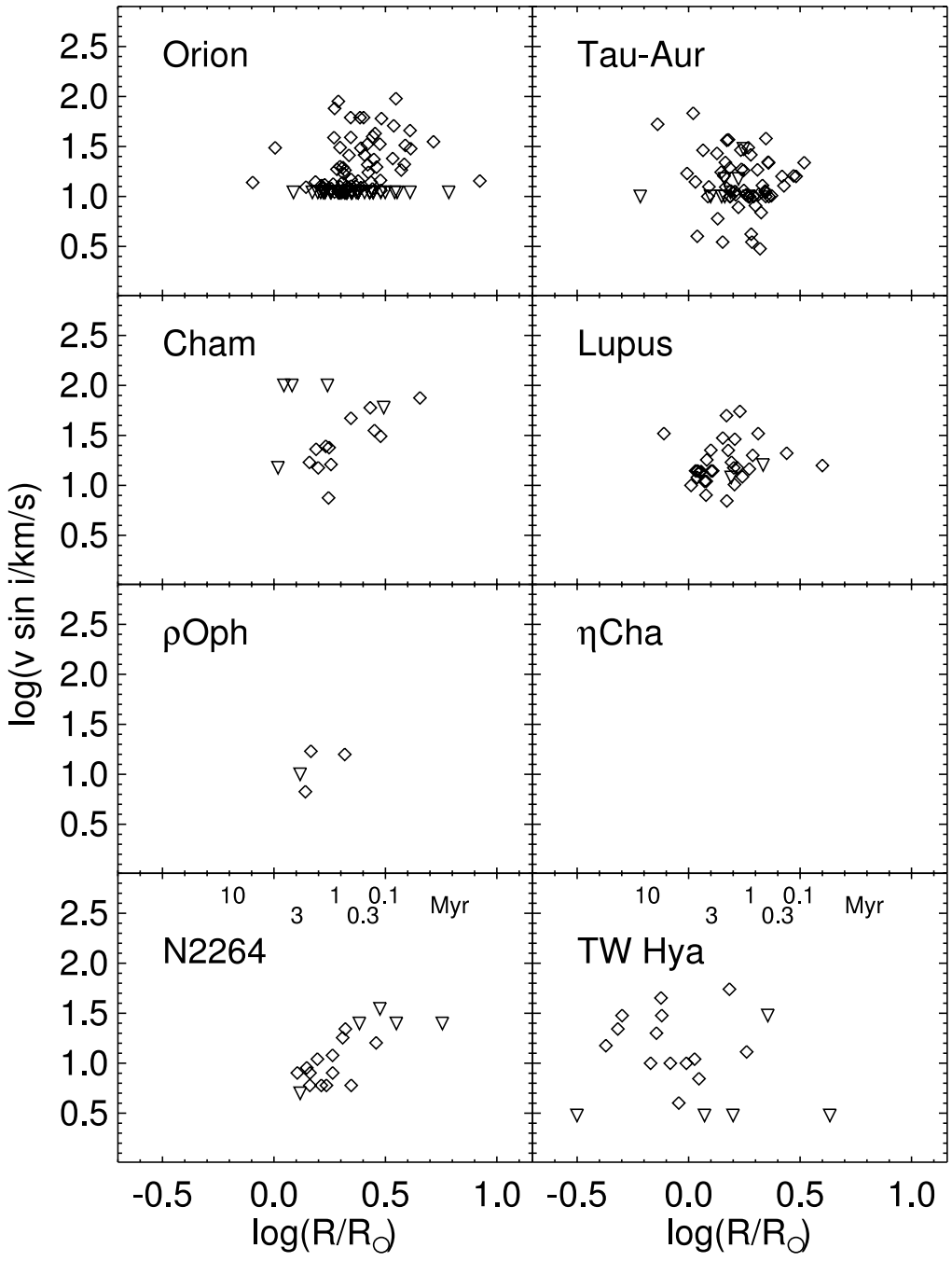

FIG. 2.—Projected rotational velocity [log ($v \sin i$)] vs. stellar radius (log R) for K5–M2 stars in eight young clusters. Approximate ages (from DAM for 0.7 $M_{\odot}$) as a function of R are indicated in the lower two panels. Upper limits are given as downward-pointing triangles. These points are averaged as a function of R in Fig. 3. Only three stars are available in ρ Ophiuchi, and no stars are available in η Chamaeleonis.

corresponds to an age range of about 0.25–5 Myr, according to the DAM models, with a few stars older and younger than this range. If we only had data for P and angular velocity were the conserved quantity, then we would expect that P would be uncorrelated with R. We would expect the same result if the errors in R were so large that we could not order the stars according to radius. However, if we have $v \sin i$ data (and if angular velocity is conserved), then we would expect $v \sin i$ to decrease in direct proportion to R. If, on the other hand, angular momentum is conserved, we expect P to increase as R^2, while $v \sin i$ varies inversely as R. Note that we do not need to know $v \sin i$ and P for the same stars; we simply need a significant number of values of $v \sin i$ and P.

The data for $v \sin i$ are shown in Figures 2 and 3. Figure 2 shows the data for all of the individual stars for each cluster. In Figure 3, we took the ensemble of all the $v \sin i$ data and calculated the mean $\log(v \sin i)$ for bins of 0.1 in $\log R$. These points are plotted in Figure 3 with error bars. The 1 σ error in the y-direction was assumed to be the standard error of the mean value of $v \sin i$. The 1 σ error in the x-direction was assumed to be half the width of the bin (larger than the scatter derived from the points in the bin). The slope of the best-fitting straight line to these mean points is 0.7 ± 0.2 and is within 2 σ of the slope of 1 expected for conservation of angular velocity. The slope is certainly inconsistent with the slope of -1 predicted for conservation of angular momentum.

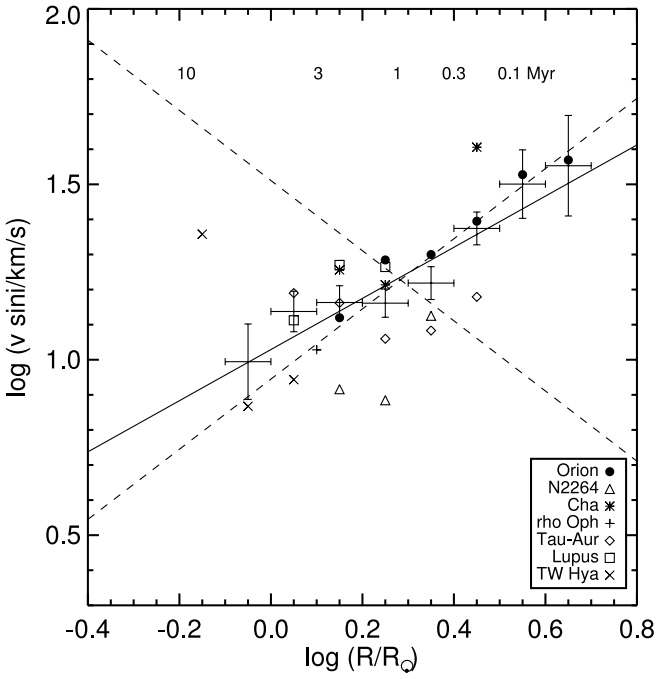

FIG. 3.—Average $\log(v \sin i)$ vs. $\log R$. The points with error bars in both directions are the average $\log(v \sin i)$ calculated for all the cluster stars within the specified range in $\log R$, and the horizontal error bars show the size of the bin. The $\log(v \sin i)$ values for each individual cluster are also plotted, provided there are at least two stars within the bin. Approximate ages (from DAM for 0.7 $M_\odot$) as a function of R are indicated. The best-fitting straight line to the entire data set is $y = 0.5(\pm 0.2)x + 1.1(\pm 0.1)$. However, the point at $\sim$10 Myr, which represents the seven oldest stars in TW Hya, deviates strongly from the trend of the other points. Although modest in number, these stars may provide the first, tantalizing hint of significant spin-up. If this point is excluded, the best-fitting straight line is $y = 0.7(\pm 0.2)x + 1.0(\pm 0.1)$ and is shown as a solid line. The dashed lines are the relationships expected for evolution with constant angular velocity (slope of 1), and conservation of angular momentum (slope of -1). The slope of the best-fitting line with the TW Hya point excluded is within 2 σ of the value expected for evolution with constant angular velocity, and either slope is inconsistent with the value expected for conservation of angular momentum.

All of the stars for which the spectral lines were unresolved and for which we have only an upper limit for $v \sin i$ have been excluded from this plot. The oldest stars plotted in Figure 3 are in the TW Hya group, and the average point for these seven stars falls well above the best-fit line for the remaining points; although modest in number, these stars may provide the first, tantalizing hint of significant spin-up. If we include this final data point, the best-fit straight line to all of the points has a slope of 0.5 ± 0.2. The slope still differs significantly from the slope of -1 required by conservation of stellar angular momentum.

In analogy to Figures 2 and 3, Figures 4 and 5 show the results for P. In Figure 5, the best-fit straight line has a slope of 0.2 ± 0.1, nearly consistent with the slope of 0 expected for conservation of angular velocity, and clearly inconsistent with the slope of 2 expected for conservation of angular momentum.

In RWSM02, we found that the distribution of $\log P$ does not change as R decreases by comparing the P distribution for the quartile with the largest radii (youngest stars) to the quartile with the smallest radii (oldest stars). In Figure 6, we similarly compare the histograms of $\log P$ obtained for different bins from Figure 5. There are enough points to make this comparison meaningful over the range $\log R \sim 0.6-0.1$. K-S probabilities enable comparisons of each of these distributions to that at $\log R = 0.2-0.1$; as can be seen from the K-S probability values indicated in the figures, the distributions are not significantly different. We chose the $\log R = 0.2-0.1$ bin as the bin to which all other distributions (including models; see below) are compared primarily because it contains a large sample of data and the distribution of P was therefore robustly determined.

In summary, the P and $v \sin i$ data sets are independently both consistent with the same hypothesis—namely, that a large fraction of PMS stars must evolve at nearly constant angular velocity during the first $\sim$4 Myr after they begin their evolution down the convective tracks. During this time, $\log R$ decreases from about 0.6 to 0.1, or by about a factor of 3. We see neither the increase in $v \sin i$ of a factor of 3 nor the decrease in P of a factor of 9 that would be expected if most stars were free to spin up and conserve angular momentum during this time. Taken together, the two data sets provide compelling evidence for the effectiveness of some mechanism that regulates the angular momentum of a large fraction of PMS stars during the first $\sim$3–5 Myr after they become observable at the stellar birthline.

However, many authors (e.g., Tinker et al. 2002, Terndrup et al. 2000, and other references in Table 8) have examined the distribution of rotational velocities among clusters with ages 30–100 Myr. These clusters contain a significant fraction ($\sim$30%) of rapidly rotating stars ($v \sin i > 50$ km s^{-1}); of the K5–M2 stars in our sample, 20% of the stars in IC 2391/2602, 37% of the stars in α Per, and 17% of the stars in the Pleiades have $v \sin i > 50$ km s^{-1}. The presence of these stars requires conservation of stellar angular momenta starting at ages $t \ll 5$ Myr. Are these results consistent with our observations?

3.3. *Hidden Effects?*

Although the ensemble trends in $v \sin i$ versus R and P versus R clearly show that the angular momenta of a large fraction of PMS stars must be regulated for ages $t < \sim 5$ Myr, the distributions are quite broad. A Gaussian fit to the $\log P$ distribution (or various subsamples thereof) produces a mean $\log P$ of 0.748 and $\sigma = 0.328$; the scatter of the $\log(v \sin i)$ data about the linear best-fit from above can also be fit by a Gaussian with $\sigma = 0.250$. The extraordinary breadth of the P and $v \sin i$ distributions at all radii (or equivalently, stellar ages for PMS stars) could well obscure evolution in these quantities for some fraction of the sample. In the discussion that follows, we develop simple models to constrain the degree of spin-up that could be hidden within the broad distribution of periods and compare the resulting limits with observations of the distribution of rotational velocities and periods in $\sim$30–100 Myr old clusters.

As discussed above, two extreme cases are likely to bracket the way in which angular momentum changes as stars evolve: (1) the stellar angular velocity is regulated by some extrinsic braking mechanism and remains constant as the star evolves; and (2) a star conserves its angular momentum, and as a result, spins up as it contracts. We can construct a simple model for how rotation rates of an ensemble of stars change with time if we assume that each star is regulated up to a specific age, after which it is released from the external braking mechanism. In order to build this simple model, we need to: (1) define the initial distribution of rotation rates; (2) determine how R changes as a function of age; and (3) set the length of time,

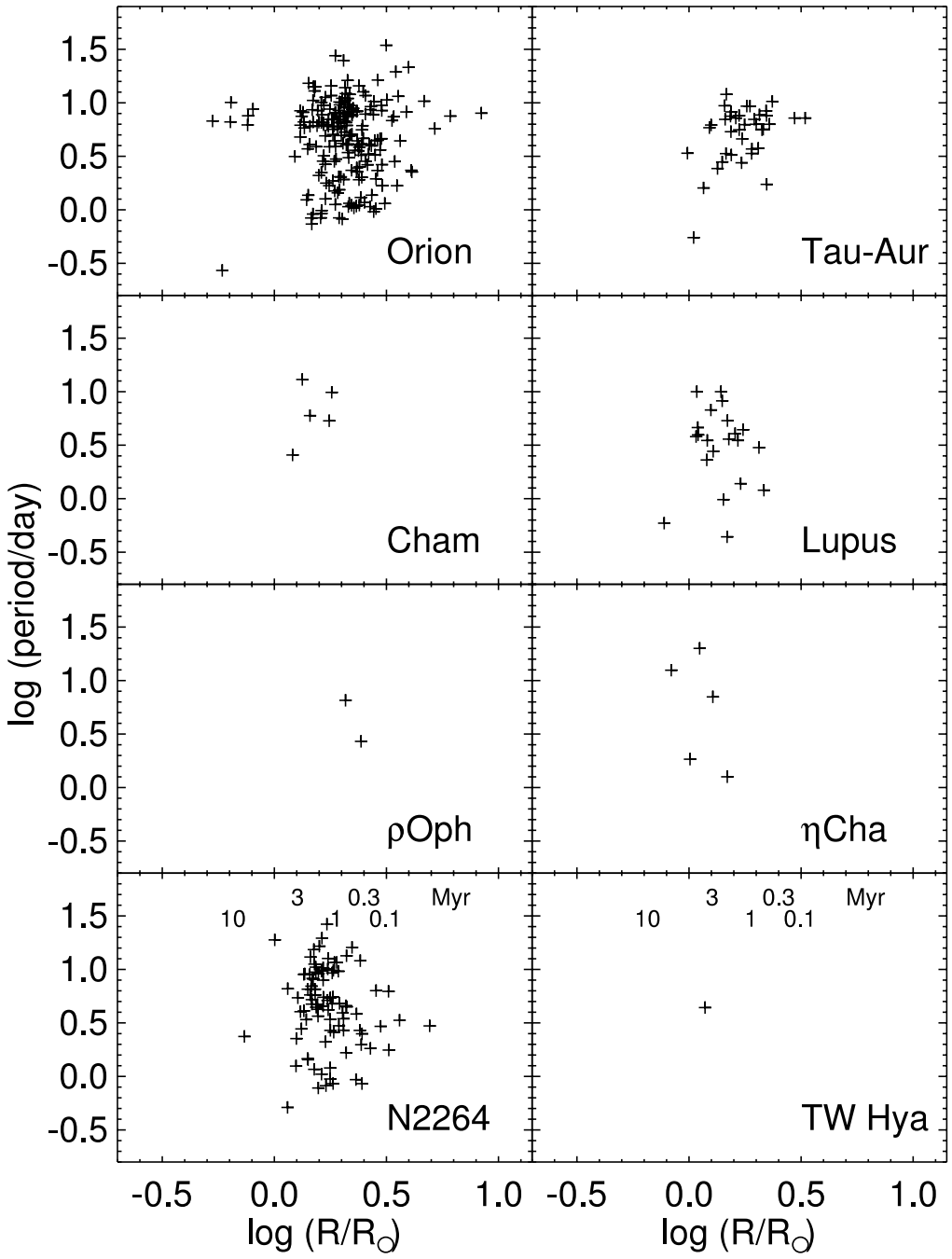

FIG. 4.—Period (log P) vs. stellar radius (log R) for K5–M2 stars in eight young clusters. Approximate ages (from DAM for 0.7 $M_\odot$) as a function of R are indicated in the lower two panels. These points are averaged as a function of R in Fig. 5. Only one star is available in TW Hya, and only two stars in ρ Ophiuchi.

which will vary from star to star, for which the external brake is effective. In constructing these models, we will consider only how P changes with time. The distribution of $\sin i$ makes the scatter in $v \sin i$ even larger than the scatter in P. Period data will therefore place tighter constraints on what fraction of the total sample of stars may be spinning up as a function of time.

In their analysis of stars with $M < 0.5\ M_\odot$, Tinker et al. (2002) assumed that the initial period distribution is Gaussian and centered on 8 days with $\sigma = 4$ days. This initial condition is similar to that assumed by Herbst et al. (2002). The distribution of P that we have found from our data set peaks at a slightly shorter period and is broader. We have, however, chosen to use the narrower, slower rotating distribution adopted by Tinker et al. in order to facilitate comparison with the other papers and because it may better represent initial conditions before any significant fraction of the PMS population has begun to spin up. Tests with simulated data show that adoption of a broader distribution does not significantly affect the results below. As in Tinker et al., we have truncated the Gaussian; we include only periods between 0.5 and 15.5 days.

Hartmann (1998) showed that for PMS stars on convective tracks, the stellar luminosity L varies approximately as $t^{-2/3}$, where t is the age of the star. Since this is a good approximation to the changes in R calculated from the DAM models,

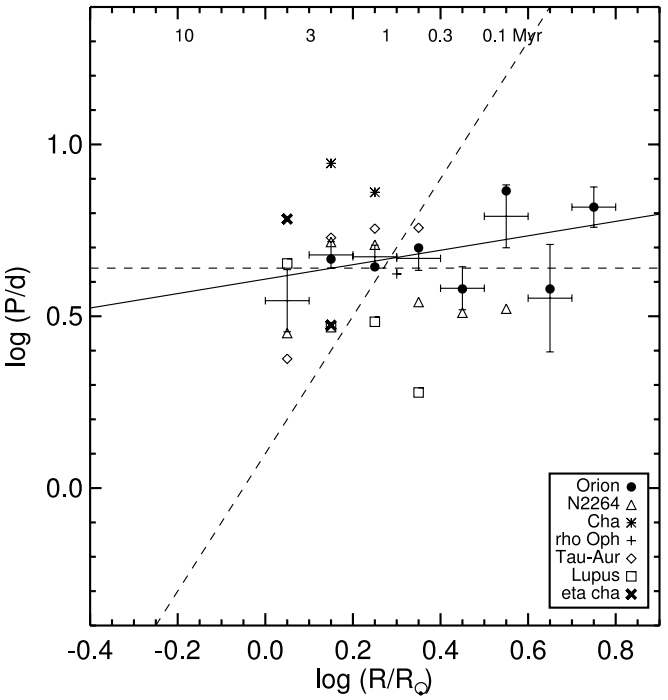

FIG. 5.— Average $\log P$ as a function of $\log R$. The points with error bars are the average $\log P$ as calculated for bins in $\log R$ for the entire ensemble data set; the error bars in the P direction are the standard error of the points in the bin, and the error bars in the R direction are the size of the bins, which is larger than the scatter in R. For comparison, average $\log P$ for each of these bins for each of the clusters (where there are more than 2 points per bin) are plotted as well. Approximate ages (from DAM for 0.7 $M_\odot$) as a function of R are indicated. The linear fit plotted here is $y = 0.2(\pm 0.1)x + 0.6(\pm 0.04)$; the correlation coefficient is 0.43. The dashed lines are the relationships expected for evolution with constant angular velocity (slope of 0), and conservation of angular momentum (slope of 2). The best-fitting line is within 2 σ of the value expected for evolution with constant angular velocity and is inconsistent with the value expected for conservation of angular momentum.

we will adopt it. After stars are released from the external regulation mechanism, P varies as R^2, so that we will assume that P varies as $t^{-2/3}$ after release.

We have considered three types of models for the evolution of P. In the first, we assume that some stars are released immediately after reaching the birthline and conserve angular momentum thereafter, while the remaining fraction of the stars are assumed to be regulated through the end of the simulation. In the second set of models, we assume that all of the rotation rates are regulated initially but that an increasing fraction of stars are released over time and allowed to spin up after release. Finally, we consider a hybrid model that includes both an immediate release of some stars and a gradual release of the remainder. Stars are selected at random from the Gaussian distribution of rotation rates to be released according to the prescriptions described above. We ran suites of simulations varying the fraction of stars released and the timing of the release. For the figures below, we have selected several of these models as representative of the rest of the simulations.

In order to make it easier to see the trends in the synthetic data in the figures, we assume a sample size of 200 stars at each of the six values of R depicted in Figures 7 and 8. The average number of stars per radius bin in our data set is smaller by a factor of 2.5. The implications of the difference in sample size per bin is discussed below.

In Figure 7, we show the results for two of our simulations in which we assume that a given fraction of the stars are released immediately and the remainder are regulated throughout. In the first, 10% of the stars are released immediately, while the remaining 90% evolve at constant P; in the second, 30% are released immediately. Histograms of $\log P$ are presented at radii comparable to those of the plots in Figure 6 to aid in direct comparison; as in Figure 6, the K-S probability that each distribution is drawn from the same population as the distribution at 1 Myr is indicated.

In Figure 7*a* (90% of the stars are regulated), we see little change between successive histograms. In Figure 7*b*, in which 30% of the stars are free to spin up, a distinctly faster rotating population is easily visible by the $\sim$1 Myr histogram. The visually apparent trend is captured quantitatively via comparison of K-S probabilities for the distributions, as noted in the figures. The combination of intrinsic breadth of the initial period distribution and the dominance of regulated stars precludes detection of "early release" stars at a statistically significant level until the released stars comprise 30% of the sample. As noted above, our assumed sample size per radius bin is 200. If we reduce the synthetic sample size to 100 per bin, which is more representative of the actual sample size in Figure 6, we cannot distinguish the "early release" stars until they comprise 40% of the population.

In addition to using K-S tests to make comparisons of two distributions, we can also use the models to derive slopes for P versus R over many values of $\log R$, as we did with our data above. Because a correlation between period and radius involves all stars in the sample rather than the smaller subsets used for the K-S comparisons, the slope provides a somewhat stronger statistical constraint than the K-S test on the fraction of stars released at the birthline. The observed slope as discussed above was 0.2 ± 0.1, which is marginally consistent with (e.g., within 2 σ of) the synthetic model that has 20% of the stars spinning up immediately and 80% of the stars still regulated at $\sim$4 Myr, and inconsistent ($\geq$3 σ) with models in which the fraction of stars released instantaneously exceeds 25%.

A notable feature of Figure 7*b* is the bimodality of the period distributions apparent at older ages. In order to obtain such a distribution, a significant fraction of stars must be free to spin up in response to contraction (i.e., released from regulation) very early ($t \ll 2$ Myr). As discussed in Herbst et al. (2000), the rate of change of the stellar radius along a PMS track for a typical low-mass star is initially very large and then slows rapidly; most of the change in stellar radius between the birthline and the ZAMS occurs by $\sim$2 Myr. Hence, early release of a fixed fraction of stars produces a bimodal distribution whose peaks are manifest at all subsequent ages (see Fig. 7); release later in the PMS phase has a far less dramatic effect on period changes, since evolution-driven changes in radius are much smaller. Herbst et al. (2002) and references therein report a statistically significant bimodal distribution in the ONC. This observation suggests that a significant population of stars in the ONC were released early and spun up in response to rapid decrease in radius over $\sim$1 Myr, while a complementary cohort remained regulated. Such bimodality is absent in the outer parts of Orion (Rebull 2001), while in other regions, the evidence is mixed (Makidon et al. 2003; Lamm et al. 2002). In ensemble, the data illustrated in Figure 6 do not show evidence for significant bimodality.

For the second set of synthetic models, seen in Figure 8, we assumed that all of the stars are regulated initially but that stars are released at a rate that varies linearly with time and,

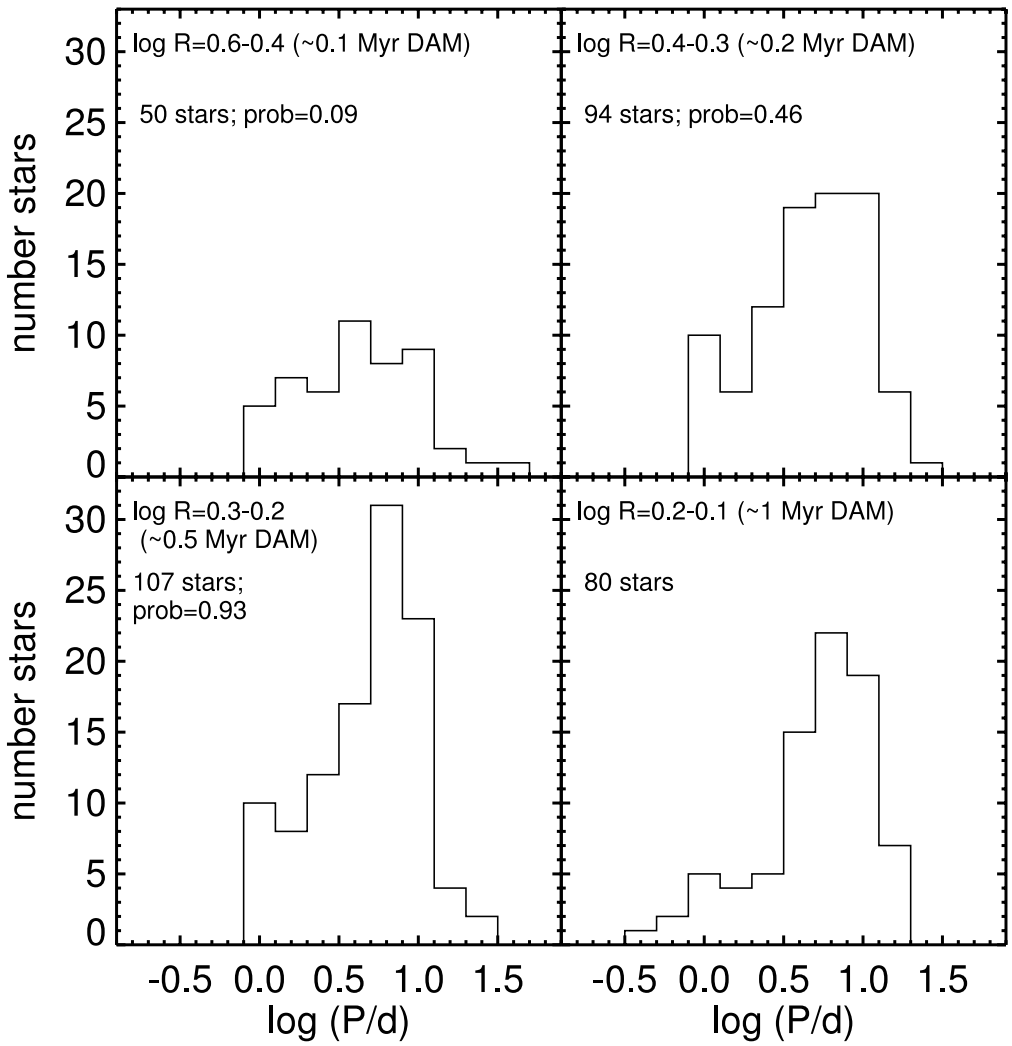

FIG. 6.—Histograms of $\log P$ as obtained for different bins in $\log R$ from Fig. 5. In each plot, the following parameters are indicated: range of $\log R$ considered, the number of stars, and the K-S probability that this distribution is drawn from the same distribution as that found in $\log R = 0.1-0.2$. According to the K-S tests, the distribution of $\log P$ does not change significantly as the stars age and R decreases.

once released, allowed to evolve thereafter while conserving angular momentum. In Figure 8, the point by which all regulated stars are released is set at radii of 1.4 and 0.8 $R_\odot$ ($\log R/R_\odot$ of 0.15 and -0.084), corresponding to approximate "cutoff ages" of about 1 and 5 Myr (according to DAM models for a 0.7 $M_\odot$ star). In Figure 8*a*, the stars are released quickly (cutoff age of 1 Myr, or half the stars released by 0.5 Myr), and the distribution rapidly becomes flatter and moves to shorter P—a result clearly in contradiction to the absence of detectable trends manifest in Figure 6. In Figure 8*b* on the other hand (cutoff age of 5 Myr, or half the stars released by 2.5 Myr), a larger fraction of stars are regulated for longer times, and the distribution does not change as rapidly.

Via comparison with the actual period distributions in Figure 6, we can reject the hypothesis that stars are released continuously from the birthline to a "cutoff" age as short as 1 Myr. However, "linear release" models in which the regulated fraction falls to zero by ages of 3 Myr or longer are consistent with the observed period distributions; the released stars are sufficiently "hidden" within the broad distribution and escape statistical detection.

If the sample size for our linear release models is decreased to a more realistic 100 stars, even a linear release model with a cutoff age as short as $t \sim 1$ Myr predicts period distributions statistically consistent (via K-S tests) with the data. However, as above, we can also calculate the $\log P$ versus $\log R$ slope for the models using a variety of $\log R$ values identical to those in the data; as noted above, this test is more robust against changes in the sample size. The slope calculated for a model with a cutoff age of 5 Myr is essentially identical to the actual slope calculated for the data. However, statistically we can also admit cutoff ages as short as 2.5 Myr or as long as 10 Myr (the endpoint of our calculation). Slopes of $\log P$ versus $\log R$ calculated from models with cutoff times less than 2.5 Myr are $\geq 3\ \sigma$ away from the slope found in the data.

Finally, we also constructed a family of models in which some fraction of the stars are released instantly at the birthline and the rest are released at a rate that is linear with time, with all of the stars being released by a certain endpoint. These "compound" models rule out scenarios in which a large fraction of the stars are released right away because, as above, stars that are released immediately undergo such rapid changes in R as they evolve that they spin up rapidly, and their period distribution becomes readily distinguishable from the rest of the ensemble of stars.

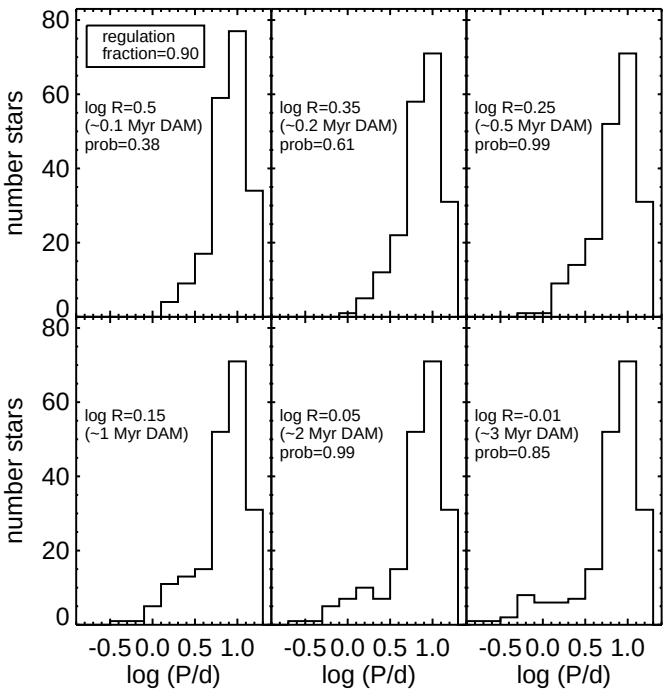

FIG. 7*a*

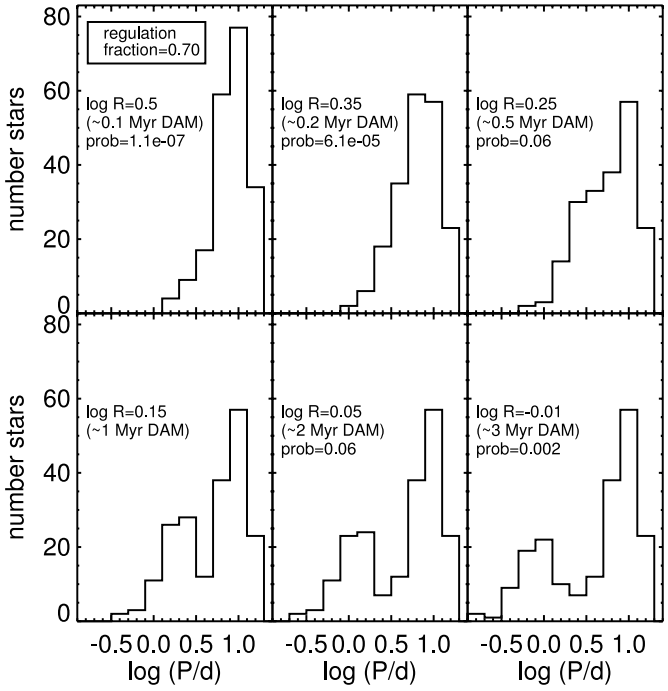

FIG. 7*b*

FIG. 7.— Histograms of $\log P$ as obtained for different bins in $\log R$ in analogy to Fig. 6, but for a Monte Carlo experiment with 200 stars in which (*a*) 10% and (*b*) 30% of the stars are released from their regulation mechanism instantly and are allowed to spin up, conserving angular momentum. In each plot (note similarity to Fig. 6), the following parameters are indicated: the $\log R$ step in the simulation and the K-S probability that this distribution is drawn from the same distribution as that found in $\log R = 0.15$. The first four histograms correspond directly to Fig. 6; two additional steps in R (or t) are provided here for clarity. In this model, the fraction of regulated stars must be $\geq$70% to be consistent with the data.

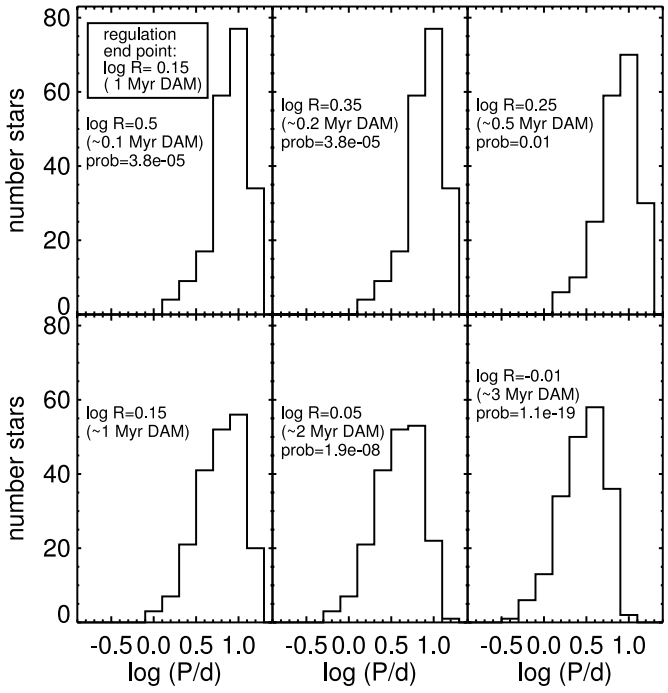

FIG. 8*a*

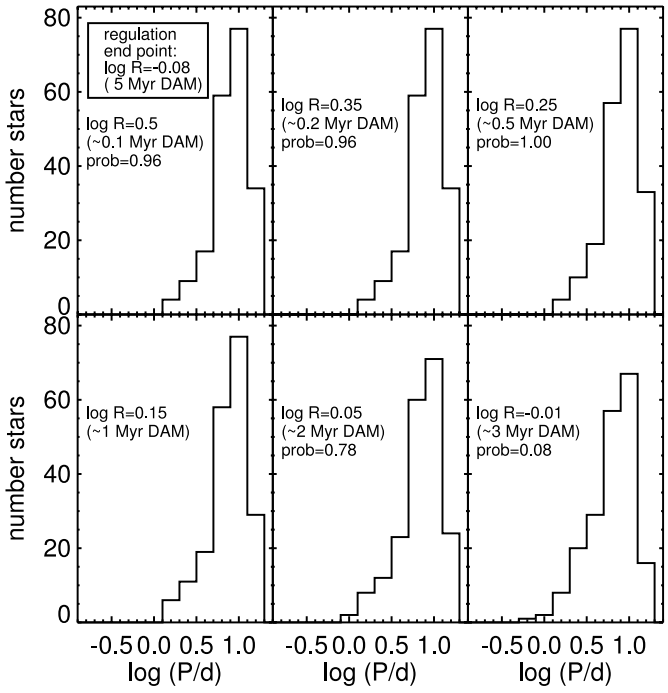

FIG. 8*a*

FIG. 8.— Histograms of $\log P$ as obtained for different bins in $\log R$ in analogy to Fig. 6, but for a Monte Carlo experiment with 200 stars in which the fraction of regulated stars falls to 0 linearly with times ending at (*a*) $\sim$1 and (*b*) $\sim$5 Myr (DAM models). When the stars are released from their regulation mechanism, they are allowed to spin up, conserving angular momentum. In each plot (note similarity to Fig. 6), the following parameters are indicated: the $\log R$ step in the simulation and the K-S probability that this distribution is drawn from the same distribution as that found in $\log R = 0.15$. The first four histograms correspond directly to Fig. 6; two additional steps in R (or t) are provided here for clarity. In this model, the regulation mechanism must last to at least 3 Myr (half the stars regulated at 1.5 Myr) to be consistent with the data.

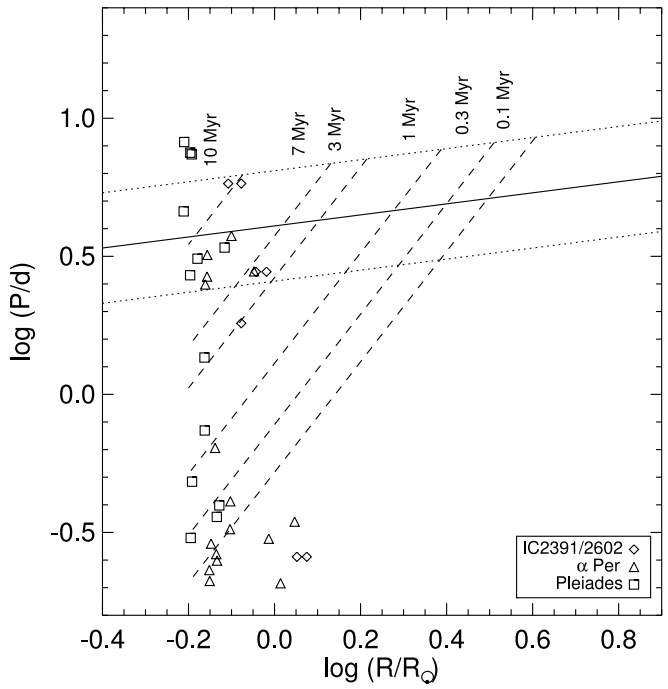

FIG. 9.—Projected rotational velocity [$\log(v \sin i)$] vs. stellar $\log R$ for stars in four older clusters. The line (with slope 0.73) is reproduced from Fig. 3; the dotted lines represent the scatter about this line found in the actual data. Approximate ages (from DAM for 0.7 $M_\odot$) are indicated as a function of R along this line. The dashed lines denote where the stars in the older clusters had to have "unlocked" in order to spin up to their current location, assuming angular momentum is conserved once rotation regulation ceases.

In summary, based on comparison of these simple simulations with the data, both via pairwise K-S comparisons between distributions and the more robust calculation of slopes of $\log P$ versus $\log R$, we conclude that (1) up to 30% of the stars could be released initially, and (2) that the regulation mechanism likely operates in some stars for ages as long as $\sim$3–5 Myr, if not longer.

3.4. *Comparison with Main-Sequence Rotation Rates*

Are these results consistent with ZAMS rotation rates in young clusters? We can make an approximate check by projecting the rotation rates observed in young clusters backward in time, while conserving angular momentum, to determine where they intercept the mean trend lines established in Figures 3 and 5. This comparison is valid, provided the angular momentum of the main-sequence stars has not changed much from the angular momentum they had when they were released from the PMS brake. A recent comparison of observations of young clusters by Barnes (2003) shows very little evolution in the distribution of P for the mass range of interest here up to the age of α Persei and only modest braking by the age of the Pleiades. Mathieu (2003) also concludes that the basic structure of the distribution is set early. Supporting evidence for little change in the rotation of MS stars over this timescale comes from Randich, Schmitt, & Prosser (1996), who find no significant difference in the distribution of X-ray luminosities of the K and M dwarfs in the Pleiades and α Persei and attribute this to the similar distribution of rotation rates of the stars in the two clusters.

Models of PMS stars in the mass range of our sample (e.g., Swenson et al. 1994) show that the moments of inertia vary as R^2 throughout PMS evolution, and so we can assume that the surface rotational velocity varies inversely with R during the portion of evolution in which angular momentum is conserved. (Wolff, Strom, & Hillenbrand [2004] have shown that decoupling takes place in stars more massive than those considered here, i.e., those with masses >1 $M_\odot$, when stars make the transition from convective to radiative tracks and that surface rotation rates vary inversely with R in PMS stars that are no longer subject to an external braking mechanism.)

Figures 9 and 10 show the P and $v \sin i$ data we culled from the literature for the K5–M2 stars in IC 2391/2602, α Persei, and the Pleiades. Stars in this spectral range span the same range of masses as the K5–M2 stars comprising our PMS sample. The estimated ages for these clusters taken from the literature are listed in Table 2.

In accordance with the discussion above, we have assumed that PMS stars, after the external brake is removed, conserve angular momentum as they complete their evolution to the ZAMS and that the rotational velocity is inversely proportional to R. In Figures 9 and 10, we have reproduced the best-fit lines to the data for young clusters from Figures 3 and 5, along with the scatter about this line due to the intrinsic range in rotation rates. We can then project the observed MS rates of rotation backward to see where they intercept the rotation rates observed for PMS stars. We see that range of rotation rates of the MS stars is consistent with the PMS data provided that some stars are released at ages <1 Myr, while a few stars must be constrained to rotate at constant velocity for 10 Myr.

We can use these data to estimate quantitatively the time over which the braking mechanism is effective in order to compare these results with the constraints derived from our analysis of PMS period distributions in § 3.3. Given the dispersion in rotation rates of PMS stars at a given value of R,

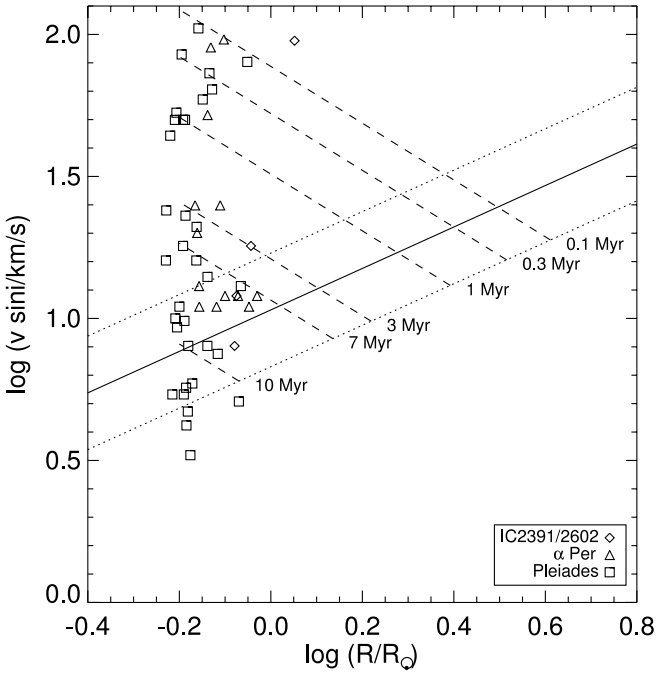

FIG. 10.—Periods ($\log P$) vs. stellar $\log R$ for stars in four older clusters. The line (with slope 0.2) is reproduced from Fig. 5; the dotted lines represent the scatter about this line found in the actual data. Approximate ages (from DAM for 0.7 $M_\odot$) are indicated as a function of R along this line. The dashed lines denote where the stars in the older clusters had to have "unlocked" in order to spin up to their current location, assuming angular momentum is conserved once rotation regulation ceases.

any given star on the main sequence could have been released from the brake at a range of possible times, as can be seen from Figures 9 and 10. Detailed modeling of the evolution of rotation of a large sample of stars that takes into account the intrinsic dispersion in angular momentum at a given mass and age has been undertaken, for example, by Herbst et al. (2002) and Tinker et al. (2002). For the consistency check we want to make, however, we can determine the *average* lifetime if we make the simplifying assumption that each main-sequence star was released at the age that corresponds to the point where the backward projection of angular momentum intercepts the best-fit line in Figures 3 and 5.

Table 5 compares the two methods of estimating the fraction of stars subject to braking as a function of age. For this table, we adopted the relationship between age and radius for a star with a mass of $\sim 0.7\ M_{\odot}$ according to the DAM tracks as being approximately midway in the mass range spanned by our sample. The second column lists the values obtained from a hybrid model (as discussed above) of the fraction of stars that are still subject to braking, on the assumption that 10% of the stars are released instantly, and the remainder of the stars are released at a rate that is linear with time, with all stars released by 5 Myr. This hybrid model reproduces the slope of the observed $\log P$ versus R plot in Figure 5. However, the data are also consistent with different rates of release for up to 30% of the stars during the first 1 Myr or with regulation times longer than 5 Myr for at least some of the stars.

The third and fourth columns in Table 5 show as a function of age the fraction of stars in which regulation continues to be effective as determined by comparing the main-sequence rotation rates and periods with the PMS trend lines in Figures 9 and 10. The range listed in Table 5 corresponds to the range in regulation fraction derived from the scatter in PMS periods on either side of the best-fit lines from Figures 3 and 5. Given the estimated uncertainties, the estimates are consistent. The comparison between main-sequence and PMS stars indicates that 25%–40% of the stars begin to spin up before they are $\sim 10^6$ yr old and about half of the stars must begin to spin up by the time they are ~ 3 Myr old. As the simple models described in § 3.3 show, the fraction that could spin up as a function of time (based on our simple models) is *consistent* with the observed period distributions of PMS stars. *Direct confirmation* of spin-up at this rate among PMS stars awaits additional observations; a sample size ~ 4 times larger than that discussed here is needed in order to diagnose spin-up with a high degree of statistical robustness.

Table 5 also indicates that no more than 10% of the stars remain regulated until they are ~ 10 Myr old. If the main-sequence stars have lost some small amount of angular momentum since they reached the main sequence from such factors as magnetic winds (e.g., Barnes 2003 and references therein), then 10 Myr should be taken as an upper limit on the time over which the braking mechanism operates.

3.5. *Comparison of Regulation Timescales with Disk Lifetimes*

The only mechanism thus far postulated to account for angular momentum loss during this phase of stellar evolution is magnetic locking to a surrounding accretion disk (i.e., Königl & Pudritz 2000; Shu et al. 2000). If this model is correct, then the observed lifetime of disks should be consistent with the constraints on the duration of the regulation mechanism as estimated in § 3.3. The proxy most frequently used to infer the presence of a disk is near-infrared excess.

A variety of authors have estimated the fraction of PMS stars that show K-band or L-band excesses as a function of age. Haisch, Lada, & Lada (2001) searched for disks in L-band and find a steep falloff of disk fraction with age. Strom et al. (1989), searching in K-band, find longer lived disks. Alves, Lada, & Lada (2000), also using K-band, find an intermediate slope for this relation. Most recently, Hillenbrand, Meyer, & Carpenter (2004), using $H-K$ excesses, find an exponential falloff of disk fraction with time.

In Table 5, we compare our estimates of the survival time of the regulation mechanism with the results from two of the surveys from the literature listed above. We adopted the literature results as reported, without adjustments for sensitivity or the difference in completeness depending on whether K or L was measured. We also accepted the reported ages without attempting to put them on a common scale, given the inherent uncertainties in assigning a single age to an entire cluster.

Some caveats are in order. Hillenbrand et al. (2004, in preparation) find a large dispersion at any given age in the frequency of inner circumstellar accretion disks. Moreover, the fraction of stars inferred to have disks if L-band data are available is substantially higher than if only K-band fluxes have been measured (e.g., Lyo et al. 2003). Furthermore, the fraction of stars with reported L-band excesses may also depend on the distance of the cluster and the detection threshold for a particular L-band survey (Lyo et al. 2003). Finally, the ages of stars in a given cluster span a million or more years, and so a single age may not adequately represent the diversity of stars in a cluster; absolute ages assigned also depend on the PMS models chosen. Despite all these concerns, the various disk fractions are reasonably consistent with one another and with the estimates in the present paper for the length of time over which the regulation mechanism is effective.

TABLE 5
Fraction of Stars with Regulation

Age DAM (Myr)	From Hybrid with 5 Myr Cutoff [a]	Range from $v \sin i$ Data	Range from P Data	Haisch et al. 2001	Hillenbrand et al. 2004
0.1	0.90	0.86–1.00	0.58–0.86	...	...
0.3	0.86	0.80–0.98	0.53–0.75	...	0.85
1	0.73	0.71–0.86	0.50–0.58	0.90	0.55
3	0.37	0.49–0.71	0.36–0.50	0.50	0.30
7	0.00	0.31–0.69	0.25–0.50	0.00	0.10
10	0.00	0.08–0.33	0.08–0.33	0.00	0.00

[a] These values are the fraction of stars requiring regulation as derived from a hybrid model with 10% of the stars released instantly and the remainder of the stars released at a rate that is linear with time with all stars released by 5 Myr (see text).

These crude estimates for the duration of regulation are also approximately consistent with previous theoretical treatments. Through detailed modeling of the kind that is appropriate to a full treatment of the physics involved in the evolution of angular momentum of stars with masses in the range 0.2–0.5 $M_{\odot}$, Tinker et al. (2002) conclude that in order to derive the distribution of rotational velocities seen in the Pleiades from the distribution seen in the ONC, it is necessary to assume that angular momentum is lost through the interaction of the protostars with their accretion disks. They found that either a fixed disk lifetime of 3 Myr for all stars or a distribution of lifetimes in the range 0–6 Myr can account for the observations. In a study of disk lifetimes in Taurus, Armitage, Clarke, & Palla (2003) conclude that about 30% of stars lose their disks within 10^6 yr, while the remainder have lifetimes in the range 1–10 Myr, and attribute the dispersion in disk lifetimes to a dispersion in the initial masses of the disks. Both the above papers yield results consistent with the constraints derived in § 3.3.

3.6. *Disked versus Nondisked Stars*

The primary argument against disk locking as the regulation mechanism has been the lack of a tight correlation between rotation rates of individual stars and the presence or absence of disk indicators, such as a near-IR excess. For example, many of the rotation surveys have attempted unsuccessfully to find differences in the period distributions between disked and nondisked stars.

With our simulations, we can determine the conditions under which we could expect to detect significant differences in period distributions between stars that have or lack disk signatures. If we assume that the regulation mechanism is indeed disk locking, then for our synthetic data, we have perfect knowledge of the disk fraction: a "regulated" star has a disk, while a "released" star lacks a disk.

If an initial percentage of stars is released immediately (i.e., for the sake of this discussion, "nondisked"), then this "nondisked" population of stars is free to spin up and diverges quickly from the regulated ("disked") sample. A K-S test can easily distinguish the period distributions of the two populations provided that it is known a priori which stars belong to which samples. However, the "tail" of fast rotators (nondisked or released population) does not become visually distinct from the main population until at least ~1 Myr. If the stars are released at a rate that is linear with time and at least some stars are regulated to at least ~5 Myr, then the distributions of periods for released (nondisked) and locked (disked) stars are not easily distinguished at any age, even for large sample sizes and with perfect knowledge of which stars are still locked and which are not. If the stars are released more slowly or there are many fewer stars available (as is the case for actual data), then the *populations are never distinguishable*, even for this case of perfect knowledge of the disked (regulated) fraction. The reason that it is so difficult to distinguish between the period distributions for regulated (disked) stars and unregulated (nondisked) stars in our models is straightforward: the broad distribution of periods obscures the differences unless (1) the sample is very large, or (2) a significant fraction of stars are released early, thereby producing large differences in mean periods between the regulated and unregulated samples. (The latter may describe the ONC, where Herbst et al. [2002] report a statistically significant difference in the period distribution between stars showing near-IR excesses and those that lack such excesses—a result that is consistent as well with the appearance of a bimodal period distribution for the ONC.)

In reality, we do not have perfect knowledge of which stars have disks, and thus are likely to still be regulated under the current formalism, and which do not. Hillenbrand et al. (1998) argue that as many as one-third of the stars with disks may have no discernible near-IR excesses and may be misclassified as lacking disks as a result of, e.g., inner disk holes and inclination effects. Again using our simulations as described above for stars that are released at a rate linear with time (with at least some stars regulated to ~5 Myr), we randomly selected 30% of the regulated stars to be misidentified as unregulated. In that case, ~400 stars per bin of $\log R$ are required to be able to reliably distinguish (via K-S tests) the period distribution of the disked from the nondisked stars. Even combining stars from multiple clusters, we are at least a factor of 4 below the required sample size. This likely explains why investigators have not yet found clear differences between period distributions for stars with and without disk signatures. Our simple simulation suggests that complete surveys of at least 4 times the sample that we have now are required in order to see clear differences between the disked and nondisked period distributions.

We finally note that another factor that may weaken any correlation between IR excess and rotation rate is the timescale required to establish disk locking relative to the evolutionary timescale for these low-mass PMS stars. If the disk locking timescale exceeds the stellar evolutionary timescale, as it may, especially for low-mass PMS stars, rotation will not correlate in a simple way with the presence or absence of a disk. Hartmann (2002) has estimated the time scale for disk braking and finds the following relationship:

$$\tau_{\rm DB} \gtrsim (4.5 \times 10^6 \text{ yr}) M_{0.5} \dot{M}_{-8}^{-1} f, \quad (6)$$

where $M_{0.5}$ is the stellar mass in units of 0.5 $M_{\odot}$, $\dot{M}_{-8}$ is the mass accretion rate in units of the typical value of 10^{-8} $M_{\odot}$ yr^{-1} observed in T Tauri stars, and f is the ratio of the actual rotation rate to the breakup velocity, with a typical value of 0.2 (e.g., Wolff et al. 2004). For T Tauri stars with a mass of 0.3 $M_{\odot}$ and a mass accretion rate of $10^{-8.6}$ $M_{\odot}$ yr^{-1}, Hartmann derives a braking timescale of 10^7 yr, concluding that locking is marginal at ages $< 10^6$ yr. Our stars are more massive than 0.3 $M_{\odot}$ and, moreover, may have larger accretion rates, because there is evidence that accretion rates increase with mass (e.g., Muzerolle et al. 2003) and decrease with time (e.g., Armitage et al. 2003). If from these papers, we adopt a mass accretion rate of 3×10^{-8} $M_{\odot}$ yr^{-1} as fairly reasonable for PMS stars in our mass and age range, the braking timescale is ~420,000 yr. Disk braking then appears to be a plausible regulation mechanism for PMS stars in the mass range 0.3–1 $M_{\odot}$ and with ages $<10^6$ yr. It must be stressed, however, that the timescale estimate is very sensitive to the mass accretion rate, which may vary by an order of magnitude at any given mass and which is, in any case, very poorly known.

4. CONCLUSIONS

To investigate what happens to angular momentum during the earliest observable phases of stellar evolution, we searched the literature for periods (P), projected rotational velocity ($v \sin i$), and supporting data on K5–M2 stars from eight young clusters. We used the observationally derived stellar R

(as determined from L_{bol} and T_{eff}) to examine two extreme cases, conservation of stellar angular velocity and conservation of stellar angular momentum.

The P and $v \sin i$ data sets are independently consistent with the same hypothesis—namely, that a significant fraction of PMS stars evolve at nearly constant angular velocity during the first $\sim$3–5 Myr after they begin their evolution down the convective tracks, despite the fact that the radius decreases by about a factor of 3 during this time. These data provide compelling evidence for the effectiveness of some mechanism that regulates the angular momentum of a significant fraction of PMS stars during the first $\sim$3–5 Myr after they become observable.

This result seems surprising at first glance, because observations of young main-sequence stars reveal a population (30%–40%) of rapidly rotating ($v \sin i > 50$ km s^{-1}) stars that must begin to spin up at ages $\ll 5$ Myr. To determine whether these apparently contradictory results are reconcilable, we use simple models along with our data set to place limits on (1) the fraction of PMS stars that must be regulated, and (2) the complementary fraction that could spin up as a function of time, but escape statistical detection given the broad distribution of stellar periods. We find that a modest fraction (30%–40%) of PMS stars could be released within the first 1 Myr and still produce period distributions statistically consistent with the observed data. This population is large enough to account for the population of rapid rotators observed among young main-sequence stars of comparable mass. Among our suite of simple models, one that assumes a linear decrease in the fraction of regulated stars as a function of time with half the stars still regulated at 2.5 Myr, best matches the formal linear relationship between mean period and time. Models with a linear decrease in the fraction of regulated stars for which all the stars are released in times as short as 2.5 Myr lie within the range permitted by statistical comparison of the models and observations.

The timescales over which stellar angular momentum regulation could be effective, as constrained by the current data set, are consistent with the lifetimes of disks as judged from the fraction of PMS stars that exhibit near-infrared excesses as a function of age. This result is thus consistent with the hypothesis that stellar angular momentum is regulated by circumstellar accretion disks that "lock" stars to rotate at an angular velocity fixed by the stellar mass, radius, the strength of the stellar magnetic field, and the mass accretion rate through the disk.

The primary argument against the hypothesis that disk locking regulates PMS star rotation rates, has been the lack of a tight correlation between rotation rates and the presence of disk diagnostics, such as a near-IR excess. We show through simulations that the intrinsic distribution of periods is so broad that, even with perfect knowledge about disks from the simulated data, a sample size of many hundreds of stars would be required to detect any correlation between P and near-IR excesses unless a large fraction of stars is released at ages $t \ll 1$ Myr. Therefore, to determine with statistical rigor whether there is a significant difference between period distributions for stars with and without disks requires very large samples; we estimate that at $\sim$1000 stars uniformly spanning radii ranging from $\log R = \sim 0.6$ to 0.1 (ages $\sim$0.1–3 Myr) are needed in order to ensure statistically robust differences.

It would also be valuable to observe rotation periods among (1) a significant population of stars with ages 7–10 Myr; and (2) additional young main-sequence stars. Comparison of (1) and (2) would constrain the level of angular momentum loss during the remaining 50% change in radius and $\sim$20 Myr between the latter PMS stages and the ZAMS. The observations of the oldest stars in TW Hya suggest that spin may be directly observable during these stages of evolution. Such data would provide much stronger constraints on the fraction of stars with long-regulation timescales.

This paper has combined data from several different regions of star formation to identify the overall trends in rotation for PMS stars. It may well be that not all regions behave in the same way. What is needed now are studies of large complete samples of stars in different regions to determine how representative the current sample is. Large sample size is clearly important in order to *define* rather than *constrain* the fraction of stars regulated and released as a function of time.

With the exception of Orion and NGC 2264, which are well sampled, the other clusters discussed here merit further observation. Those observations should include both period and $v \sin i$ observations. Clusters treated here are not completely sampled; detecting periods robustly may be biased against stars surrounded by accretion disks, and $v \sin i$ data may not find the slowest rotators.

Testing the disk-locking hypothesis requires not only large ($\sim$500–1000 stars) samples but a reliable disk indicator. The *Spitzer Space Telescope* (formerly *SIRTF*) and large ground-based telescopes should enable the high precision L-band measurements that appear to provide our best indication of whether a star is surrounded by an accretion disk. However, given the many other factors that may affect the relationship, establishing a correlation between period and disk fraction may, in the end, very well prove extremely difficult.

We wish to thank Lynne Hillenbrand for sharing early results of her work on disk fractions, and David M. Cole for a critical reading of the manuscript. L. M. R. wishes to thank both the SSC and NOAO for funding her trips to Tucson to work on this project. This research has made extensive use of NASA's Astrophysics Data System Abstract Service, and of the SIMBAD database, operated at CDS, Strasbourg, France. Part of this work was carried out while L. M. R. was a National Research Council Resident Research Associate located at the Jet Propulsion Laboratory. The research described in this paper was partially carried out at the Jet Propulsion Laboratory, California Institute of Technology, under a contract with the National Aeronautics and Space Administration.

APPENDIX A

DATA DETAILS

We searched the literature for rotation and supporting data on stars in the Orion Nebula Cluster and environs, ρ Ophiuchi, TW Hydra, Taurus-Auriga, NGC 2264, Chamaeleon, Lupus, η Chamaeleonis, IC 2391, IC 2602, α Persei, and the Pleiades. Table 6 lists all references consulted for Orion and Taurus-Auriga, Table 7 lists references consulted for the six remaining young clusters (ρ Ophiuchi, TW Hydra, NGC 2264, Chamaeleon, Lupus, and η Chamaeleonis), and Table 8 lists references consulted for the four

TABLE 6
REFERENCES FOR ROTATION AND SUPPORTING DATA: ORION AND TAURUS-AURIGA

Reference	Cluster(s)	Data Type
Bouvier 1990 [68]	Taurus-Auriga	P; $v \sin i$; types
Bouvier & Bertout 1989a, 1989b [45]	Orion, Taurus-Auriga	types; P, $v \sin i$
Bouvier et al. 1986 [44]	Orion, Taurus-Auriga	types; $v \sin i$; P
Bouvier et al. 1993 [60]	Taurus-Auriga	P; $v \sin i$; types
Bouvier et al. 1995 [61]	Taurus-Auriga	P; V, I mags; synonyms
Bouvier et al. 1997a [59]	Taurus-Auriga	P; types; V mags
Bouvier et al. 2003 [121]	Taurus-Auriga: AA Tau	P
Carpenter, Hillenbrand, & Skrutskie 2001 [4]	Orion	P
Choi & Herbst 1996 [49]	Orion	P
Chelli et al. 1999 [57]	Taurus-Auriga: DF Tau	P
Clarke & Bouvier 2000 [55]	Taurus-Auriga	$v \sin i$; synonyms
DeWarf et al. 2003 [71]	Taurus-Auriga: SU Aur	P
Duncan 1993 [51]	Orion	$v \sin i$; types; V mags
Edwards et al. 1993 [110]	Taurus-Auriga	types; P; V, I mags
Feigelson & Kriss 1981 [74]	Taurus-Auriga	V mags; types
Gagné & Caillault 1994 [included in 10]	Orion	V, I mags; types; synonyms; $v \sin i$; P
Gagné, Caillault, & Stauffer 1995 [10]	Orion	V, I mags; types; synonyms; $v \sin i$; P
Gahm et al. 1993 [123]	Taurus-Auriga	P; V, I mags; types
Gameiro & Lago 1993 [52]	Taurus-Auriga	$v \sin i$; types
Gullbring & Gahm 1996 [64]	Taurus-Auriga	P; V mags
Hartmann & Stauffer 1989 [58]	Taurus-Auriga	$v \sin i$; synonyms
Herbig & Bell 1988 [72]	Orion, Taurus-Auriga	types; $v \sin i$; V mags
Herbst & Koret 1988 [67]	Orion, Taurus-Auriga	V mags; P
Herbst & Shevchenko 1999 [63]	Orion, Taurus-Auriga	V mags
Herbst et al. 2000 [6], 2001 & 2002[2]	Orion	P
Hillenbrand 1997 [9]	Orion	V, I mags
Kenyon & Hartmann 1995 [62]	Taurus-Auriga	synonyms; types; V, I mags
Magazzù, Rebolo, & Pavlenko 1992 [124]	Taurus-Auriga	types; $v \sin i$
Montes & Ramsey 1999 [66]	Taurus-Auriga	$v \sin i$; types
Neuhäuser et al. 1995 [70]	Taurus-Auriga	$v \sin i$; P; synonyms
Neuhauser et al. 1998 [104]	Orion: Par 1724	P; $v \sin i$; V, I mags
Padgett 1996 [105]	Tau-Aur, Orion	types; some $v \sin i$
Preibisch & Smith 1997 [56]	Taurus-Auriga	P; $v \sin i$; types; binarity
Rebull 2001 [1]	Orion	P
Rebull et al. 2000 [8]	Orion	V, I mags; types
Rhode et al. 2001 [5]	Orion	$v \sin i$; P; V, I mags
Rydgren et al. 1984 [125]	Taurus-Auriga	V, I mags
Smith, Beckers, & Barden 1983 [106]	Orion	types; $v \sin i$
Stassun et al. 1999 [3]	Orion	P
Strom, Strom, & Merrill 1993 [11]	Orion	types
Strom et al. 1989 [65]	Taurus-Auriga	types; V, I mags
Vogel & Kuhi 1981 [50]	Taurus-Auriga	synonyms; types; $v \sin i$
Vrba et al. 1993 [53]	Taurus-Auriga	V, I mags; P
Walker 1969	Orion	synonyms
Walker 1983 [107]	Orion	synonyms; types
Walker 1990 [108]	Orion	P; $v \sin i$
Walter et al. 1988 [73]	Taurus-Auriga	types; $v \sin i$; V mags
White & Basri 2003 [69]	Taurus-Auriga	$v \sin i$; types
Wichmann et al. 2000 [54]	Taurus-Auriga	$v \sin i$; types; binarity
Wolff et al. 2004 [7]	Orion	$v \sin i$; V, I mags; types; synonyms

NOTE.—Reference numbers in brackets are used in Table 10.

oldest clusters (IC 2391, IC 2602, α Persei, and the Pleiades). From these references, we collected spectral types, V and Cousins I (referred to simply as I) magnitudes, periods (P), and projected rotational velocities ($v \sin i$). We also consulted the literature for ages, reddening, distances, and stellar densities (Table 2 above); Table 9 lists the references consulted for each cluster. Finally, Table 10 collects data for all of the stars used for this analysis, i.e., stars with V and I magnitudes, spectral types (with those types falling between K5 and M2), and rotational information (P or $v \sin i$).

We tried to limit the influence of possible metallicity-related effects (e.g., on the spectral type–color relation) by considering clusters of similar metallicity. Literature values were consulted for the clusters when possible (e.g., Cunha, Smith, & Lambert 1998; Padgett 1996; King et al. 2000b; Kastner et al. 2002; Prosser 1998;[4] Randich et al. 2001; Pinsonneault et al. 1998). All of the clusters are thought to be very close to solar metallicity or slightly below it (the worst case is 0.15 dex below solar).

[4] See http://www.noao.edu/noao/staff/cprosser.

TABLE 7

REFERENCES FOR ROTATION AND SUPPORTING DATA: YOUNGER CLUSTERS BESIDES ORION AND TAURUS-AURIGA

Reference	Cluster(s)	Data Type
Alcalá et al. 1995 [28], 1997 [33]	Cham	types; *V, I* mags
Batalha et al. 1998 [34]	Lupus, ρ Oph, Cham	*P*; types; synonyms
Batalha et al. 2002 [95]	TW Hya: TW Hya itself	*P*
Bouvier 1990 [68]	ρ Oph, Cham, Lupus	types; *P*; $v \sin i$
Bouvier & Appenzeller 1992 [46]	ρ Oph	*V, I* mags; types
Bouvier & Bertout 1989a, b [45]	Lupus, Cham	types; $v \sin i$; *P*
Bouvier et al. 1986 [44]	Lupus, ρ Oph, Cham	types; $v \sin i$; *P*
Carpenter et al. 2002 [29]	Cham	synonyms
Chen et al. 1997 [80]	Cham, Lupus	types
Comerón, Rieke, & Neuhäuser 1999 [41], 2000	Cham	*V, I* mags; types
Covino et al. 1992 [43], 1997 [32]	Lupus, ρ Oph, Cham	types; $v \sin i$; *V, I* mags; synonyms
Doppman, Jaffe, & White 2003 [47]	ρ Oph	$v \sin i$, types
Dubath, Reipurth, & Mayor 1996 [35]	Lupus, Cham	$v \sin i$
Edwards et al. 1993 [110]	ρ Oph, Cham, Lupus	types; *P*; *V, I* mags
Feigelson et al. 1993 [26]	Cham	synonyms
Feigelson & Kriss 1989 [30]	Cham	*V* mags; types
Flaccomio et al. 1999 [15]	NGC 2264	*V* mags; types
Franchini et al. 1988 [22], 1992 [39]	Lupus, Cham, TW Hya	types; $v \sin i$
Gauvin & Strom 1992 [23]	Cham	synonyms; *V, I* mags; types; *P*
Ghez et al. 1997 [111]	Cham, Lupus	binarity; types
Greene & Lada 1997, 2000, 2002 [116]	ρ Oph	types; $v \sin i$; *P*
Greene & Meyer 1995 [117]	ρ Oph	some types
Gregorio-Hetem et al. 1992 [76]	Lupus, ρ Oph, Cham, TW Hya	synyonyms, *V, I* mags
Gullbring & Gahm 1996 [64]	ρ Oph	*P*; *V, I* mags
Hamilton et al. 2001 [17], 2003 [21]	NGC 2264: KH15D	type, $v \sin i$
Hartigan 1993 [113]	Cham	synonyms; some *I* mags
Henize & Mendoza 1973 [38]	Cham	synonyms
Herbig & Bell 1988 [72]	Lupus, ρ Oph, NGC 2264, Cham	types; $v \sin i$; *V* mags
Herbst & Koret 1988 [67]	TW Hya	*V* mags; *P*
Herbst & Shevchenko 1999 [63]	Lupus, ρ Oph, NGC 2264	*V* mags
Huenemoerder, Lawson, & Feigelson 1994 [31]	Cham	types; synonyms
Hughes & Hartigan 1992 [24]	Cham	*V, I* mags; types
Hughes et al. 1994 [77]	Lupus	*V, I* mags; types
Jayawardhana, Monhanty, & Basri 2002 [118]	ρ Oph	types; $v \sin i$
Joergens & Guenther 2001 [36]	Cham	$v \sin i$; *P*; synonyms
Joergens et al. 2001 [78]	Lupus: RX J1608.6-3922	$v \sin i$; *P*
Kearns & Herbst 1998 [19]	NGC 2264	*P*
Krautter et al. 1997 [84]	Lupus	types; *V* mags
Lawson, Feigelson, & Huenemoerder 1996 [27]; Lawson et al. 2002 [85]	Cham, η Cha	*V, I* mags; types; synonyms
Lawson et al. 2001 [86]	η Cha	*P*; $v \sin i$
Luhman & Rieke 1999 [119]	ρ Oph	types
Magazzù et al. 1992 [40]	Lupus, ρ Oph, Cham	types; $v \sin i$
Makidon et al. 2003 [18]	NGC 2264	*P*
Mamajek, Lawson, & Feigelson 1999	η Cha	synonyms; types
McNamara 1990 [16]	NGC 2264	$v \sin i$; types
Montmerle et al. 2000 [120]	ρ Oph	*P*
Neuhäuser & Comerón 1999 [114]	Cham	types; *I* mags
Padgett 1996 [105]	Cham, ρ Oph	types; some $v \sin i$
Park et al. 2000 [14]	NGC 2264	*V, I* mags; types
Petr et al. 1999 [79]	Lupus	*P*
Rebull et al. 2002b [12]	NGC 2264	*V, I* mags; types
Reid 2003 [96]	TW Hya	*V, I* mags; types
Schwartz 1977 [37]	Cham, Lupus	synonyms
Shevchenko & Herbst 1998 [42]	ρ Oph	*P*
Soderblom et al. 1999 [20]	NGC 2264	$v \sin i$; synonyms; binarity
Song et al. 2002 [91]	TW Hya	$v \sin i$; synonyms
Sterzik et al. 1999 [93]	TW Hya	*V* mags; types; $v \sin i$
Sung et al. 1997 [13]	NGC 2264	*V, I* mags; types
Torres et al. 2001 [88], 2003 [92]	TW Hya	*V* mags; types; $v \sin i$
Vogel & Kuhi 1981 [50]	NGC 2264	synonyms; types; $v \sin i$
Walter 1992 [25]	Cham	synonyms
Walter et al. 1994 [48]	ρ Oph	*V, I* mags; synonyms; $v \sin i$; types
Webb et al. 1999 [94]	TW Hya	types; synonyms
Whittet et al. 1997 [115]	Cham	types; *V* mags; synonyms
Wichmann et al. 1997 [83], 1998b [82], 1999 [75]	Lupus	synonyms; types; *V* mags; $v \sin i$; *P*
Zuckerman et al. 2001 [89]	TW Hya	types; *V, I* mags

NOTE.—Reference numbers in brackets are used in Table 10.

TABLE 8

REFERENCES FOR ROTATION AND SUPPORTING DATA: OLDER CLUSTERS

Reference	Cluster(s)	Data type
Balachandran, Lambert, & Stauffer 1988, 1996 [130]	α Per	V mags; $v \sin i$
Barnes et al. 1999 [90]	IC 2602	P; $v \sin i$
Barnes et al. 2001 [131]	α Per	P; $v \sin i$
Basri & Martin 1999 [132]	α Per	V, I mags; $v \sin i$
Boesgaard, Armengaud, & King 2003 [140]	Pleiades	$v \sin i$
Bouvier 1996 [133]	α Per	P; V, I mags; $v \sin i$
Bouvier et al. 1998 [141]	Pleiades	I mags; synonyms
James et al. 2000 [99]	α Per, IC 2391/2602	types; P; V, I mags
King, Krishnamurthi, & Pinsonneault 2000a [142]	Pleiades	V, I mags; P; synonyms
Marino et al. 2003 [109]	IC 2391: VXR 45	P
Messina 2001 [103]	α Per, Pleiades	P; V, I
Messina, Rodonò, & Guinan 2001 [101]	IC 2391, IC 2602, α Per, Pleiades	P, $v \sin i$
O'Dell & Collier-Cameron 1993 [134]	α Per	P
O'Dell et al. 1997 [135]	α Per	P
Patience et al. 2002 [136]	α Per	synonyms; V mags; types; $v \sin i$
Patten & Simon 1996 [112]	IC 2391	P; $v \sin i$; types; V, I mags
Pizzolato et al. 2003 [126]	IC 2391, IC 2602, α Per, Pleiades	V mags; P
Prosser 1998 [97]	IC 2391, IC 2602, α Per, Pleiades	V, I mags; types; P; $v \sin i$
Randich et al. 1996 [137]	α Per	$v \sin i$
Randich et al. 1997 [127]	IC 2602	types; V, I mags; $v \sin i$
Randich et al. 1998 [100]	α Per	$v \sin i$; types
Randich et al. 2001 [98]	IC 2602/2391	V, I mags; $v \sin i$
Stauffer et al. 1985, 1989 [138]	α Per	V, I mags; $v \sin i$; P
Stauffer et al. 1997 [128]	IC 2391/2602	V, I mags; $v \sin i$
Stauffer et al. 1999 [139]	α Per	I mags; types
Terndrup et al. 1999 [143], 2000 [102]	Pleiades	V, I mags; $v \sin i$
Tschape & Rudiger 2001 [129]	α Per, IC 2602, Pleiades	synonyms; types

NOTE.—Reference numbers in brackets are used in Table 10.

TABLE 9

REFERENCES FOR AGES, REDDENING, DISTANCES, AND STELLAR DENSITIES

Cluster	References
Orion	Walker 1969, Warren & Hesser 1978, Genzel et al. 1981, Hillenbrand 1997, Rebull et al. 2000
Cham	Whittet et al. 1987, 1997, Prusti, Whittet, & Wesselius 1992, Lawson et al. 1996, Knude & Hog 1998, Bertout et al. 1999, Comerón, Neuhäuser, & Kass 2000, Kenyon & Gomez 2001, Neuhäuser et al. 2002
ρ Oph	de Geus et al. 1989, Knude & Hog 1998, Martin et al. 1998, de Zeeuw et al. 1999, Bertout et al. 1999, Montmerle et al. 2000, Luhman et al. 2000
NGC 2264	Sung et al. 1997, de Zeeuw et al. 1999, Park et al. 2000, Rebull et al. 2002b, Haisch et al. 2001
Tau-Aur	Kenyon & Hartmann 1995, Preibisch & Smith 1997, Bouvier et al. 1997a, Bertout et al. 1999
Lupus	Hughes et al. 1993, 1994, Tachihara et al. 1996, 2001, Wichmann et al. 1997, Rizzo et al. 1998, Bertout et al. 1999, de Zeeuw et al. 1999, Crawford 2000, Franco 2002
η Cha	Mamajek et al. 1999, Mamajek, Lawson, & Feigelson 2000, Lawson et al. 2001, 2002, Lyo et al. 2003
TW Hya	Webb et al. 1999, Bertout et al. 1999, Sterzik et al. 1999, Torres et al. 2001, Song et al. 2002
IC 2391/2602	Stauffer et al. 1997, Pinsonneault et al. 1998, Prosser 1998, van Leeuwen 1999, Barrado y Navascués, Stauffer, & Patten 1999
α Per	Soderblom et al. 1993, Prosser 1998, Stauffer et al. 1999, de Zeeuw et al. 1999, van Leeuwen 1999
Pleiades	O'Dell et al. 1994, Pinsonneault et al. 1998, Prosser 1998, van Leeuwen 1999

TABLE 10
DATA VALUES ADOPTED OR DERIVED FOR ANALYSIS[a]

Cluster	Star Name[b]	Spectral Type	$\frac{R}{R_\odot}$	$v \sin i$ (km s^{-1})	Period (days)	References
Orion	H97: 3020	M0.5	4.0	...	21.45	1, 8, 9
Orion	H97: 3110	K6e	1.6	...	0.84	2, 9
Orion	H97: 3126	K7	1.6	...	8.46	2, 8
Orion	H97: 3151	M1	2.3	...	3.24	1, 8
Orion	H97: 5078	K7	2.3	...	2.46	3, 8

NOTE.—The complete version of this table is in the electronic edition of the Journal. The printed edition contains only a sample. Reference numbers listed in this table correspond to the bracketed numbers and associated references listed in Tables 6, 7, and 8. The additional references in Tables 6–8 provide links to papers containing information either for stars outside the K5–M2 range used in our analysis or stars having rotation measures but missing photometry or types.

[a] Includes K5–M2 stars with available rotation information and V and I magnitudes.

[b] Nomenclature notes.— Frequently used names are listed in all cases. For additional clarity, we note the following: for Orion, H97 numbers are from Hillenbrand 1997 and R01 numbers are from Rebull 2001; for NGC 2264, R numbers are from Rebull et al. 2002b.

A1. ORION

The Orion Nebula Cluster (ONC) is nearby (470 $\pm$ 70 pc), compact (size $\sim$1 pc), and young (typical stellar ages of $\sim$1–3 Myr; see, e.g. Hillenbrand 1997). The Orion Flanking Fields (FFs) surround the Trapezium region and were defined and studied by Rebull et al. (2000) and Rebull (2001). Stars in these fields that have characteristics of young stars are thought to be associated with the ONC for several reasons discussed in RWSM02, Rebull et al. (2000), and Rebull (2001). Therefore, we adopt the same distance for stars in the ONC and the FFs. The interstellar reddening toward stars in the ONC has been demonstrated to be particularly patchy, whereas it is less clumpy toward the FFs.

Distance determinations for the ONC range from 480 $\pm$ 100 pc found 25 yr ago by Warren & Hesser (1978) to 381 $\pm$ 70 pc found using *Hipparcos* data by Bertout, Robichon, & Arenou (1999). A commonly adopted value is 470 $\pm$ 70 pc (Genzel et al. 1981). We adopted this distance as a value near the middle of recent distance determinations.

The ONC itself is an extremely dense star-forming region, with O and B stars creating an H II region. The star number density can exceed 10^4 pc^{-3} (Hillenbrand 1997, Hillenbrand & Hartmann 1998). The FFs are much less dense, although clearly related to the ONC population, as the surface density found in the outer reaches of the ONC is well matched by the FFs (Rebull et al. 2000); the number density is $\sim 10^3$ pc^{-3}. Although the stars in the FFs are in a different environment than the ONC, the populations are indistinguishable in numerous ways (e.g., mass and age distributions; Rebull et al. 2000). In the whole ONC region, there is perhaps $\sim$1800 $M_\odot$ in stars, with several thousand $M_\odot$ in gas and dust.

Orion is clearly the best represented of all of the clusters discussed here, with rotation information, spectral types, and V and I magnitudes for $\sim$600 stars. Extensive discussion on reddening and reddening corrections was included in Rebull et al. (2000) and Rebull (2001), so we do not repeat it here. The existing rotation surveys of Orion are perhaps the most complete for any young cluster.

A2. CHAMAELEON

This southern hemisphere cloud complex involves at least two clouds, called Cha I and II, which we group together for our purposes here. The complex may include Cha III, but we do not include that cloud here, nor do we assume the η Chamaeleonis cluster is at this same distance; see below. There seems to be very little reddening between Earth and the T Tauri stars, although there are many embedded cloud cores.

The distance to these clouds is controversial, with some authors determining that both clouds are about the same distance and others concluding that Cha II is significantly more distant. Various authors using *Hipparcos* results (e.g., Bertout et al. 1999; Knude & Hog 1998) obtain values for both Cha I and II of $\sim$160 $\pm$ 20 pc, consistent with older determinations (e.g., Whittet et al. 1987, 1997). We use a value of $\sim$160 $\pm$ 20 pc here.

The star-forming environment found here is similar to that in Taurus-Auriga; it is a less dense region, with very few O and B stars. The cloud mass in Cha I and II is $\sim$2000 $M_\odot$, with roughly 2 to 3 T Tauri stars found per pc^3 (Mizuno et al. 1999; Tachihara et al. 2001). The T Tauri stars in this cluster are so dispersed that this region has been used to support theories of local formation of isolated T Tauri stars (Tachihara et al. 2001).

There are about 40 stars with rotational information, spectral types, and V and I magnitudes available in the literature for Chamaeleon. In the process of rederiving reddening for each star, we found apparently negative reddening for only 2 stars, and for those, we used the most likely reddening of $A_I = 0.92$. Stars with $v \sin i$ here outnumber stars with P by $\sim$3:1, and most of the stars with P also have known $v \sin i$.

A3. ρ OPHIUCHI

This cluster has many stars still deeply embedded in natal material (e.g., YLW 15, WL 6), but there are also known T Tauri stars.

Various authors have obtained distances ranging from 125–165 pc. Of the closer distances, Bertout et al. (1999) find 128 $\pm$ 11 pc, Knude & Hog (1998), 120 pc, and de Geus, de Zeeuw, & Lub (1989), 125 $\pm$ 25 pc. At the other extreme, Montmerle et al. (2000) find 160 pc; de Zeeuw et al. (1999) find a middle range value of 145 pc. We selected 130 pc as an approximate weighted average.

Allen et al. (2002) find peak stellar densities for this cluster similar to that found by Hillenbrand & Hartmann (1998) for the Trapezium. Note, however, that the central ONC region is much ($\sim 10\times$) larger than the central region of ρ Ophiuchi.

There are fewer than 10 stars with rotational information, spectral types, and V and I magnitudes available in the literature for this cluster, several of which are more embedded than classical T Tauri stars (CTTS). In the process of rederiving reddening, all of the stars had physically reasonable reddening values. Half of the sample has P, and the other half has $v \sin i$. Although Shevchenko & Herbst (1998) reported periods for several more stars than this, our requirement that the stars also have spectral types and V and I magnitudes forced us to drop those stars from our final database.

Specifically in the context of disk lifetimes, we mention here for completeness that Wilking et al. (2001) conclude that disks in this cluster may have shorter-than-average survival times.

A4. NGC 2264

NGC 2264, part of the Mon OB 1 association, is about twice as far away as Orion; we used a distance modulus of 9.40, or 760 pc (Sung, Bessell, & Lee 1997). de Zeeuw et al. (1999) summarize a previously known distance and age of $\sim$950 pc and $\sim$3 Myr. Of five stars in the *Hipparcos* database that are also in NGC 2264, they found four to have parallaxes of larger than 2.5 mas, i.e., a distance less than 400 pc, which is much smaller than previous estimates.

As in Orion, a molecular cloud located behind the cluster aids in blocking background field stars and limiting the cluster depth to a small fraction of the distance to the cluster. The total cloud mass is $\sim 10^3\ M_\odot$. A total cluster mass awaits more complete membership surveys, but the surface density of stars here is much less dense than the ONC; making some simple assumptions suggests ~ 1 star pc^{-3}.

This cluster is fairly well represented here, with rotation information, spectral types, and V and I magnitudes for $\sim$150 stars. Extensive discussion on reddening and reddening corrections was included in Rebull et al. (2002b), so we do not repeat it here. Stars with P outnumber stars with any $v \sin i$ information by about a factor of 2. There are only about 20 stars for which there are both P and $v \sin i$ data currently available, and many of those $v \sin i$ values are only upper limits. The range of rotation rates covered by $v \sin i$ is not as large as those with P, an obvious direction for future work.

A5. TAURUS-AURIGA

Taurus-Auriga is a very well studied region, often held up as the canonical low-density star-forming region with 1–10 stars pc^{-3}. Kenyon & Hartmann (1995) find that most stars are younger than 2 to 3 Myr, assuming a distance of 140 ± 10 pc as found by Kenyon, Dobrzycka, & Hartmann (1994). Bertout et al. (1999), based on *Hipparcos* data, find a value very close to that of 139 ± 10 pc. Using only their most reliable parallaxes, they find three distinct groups at 125 ± 18, 140 ± 15, and 168 ± 35 pc. Preibisch & Smith (1997) used rotational information to constrain the distance to and width of the cluster to be 152 ± 10 and 20 pc, respectively. For our purposes here, we used 140 pc.

There are about 120 stars with rotational information, spectral types, and V and I magnitudes available in the literature for Taurus-Auriga. In the process of rederiving reddening, we found apparently negative reddening for less than 10% of the sample, and for those stars, we used a most likely reddening of $A_I = 0.37$. There are both P and $v \sin i$ available for about half the sample, thanks to efforts by Bouvier and collaborators.

A6. LUPUS

The Lupus cloud complex is composed of at least five subgroups (see, e.g., Tachihara et al. 1996, 2001), which we group together here. However, the distance to this cluster is controversial. Hughes, Hartigan, & Clampitt (1993) conclude that the distance to the cluster is 140 ± 20 pc, which is also obtained by Bertout et al. (1999) and de Zeeuw et al. (1999), both independently using *Hipparcos* data, although admittedly via only a few stars. Different distances have been obtained by Crawford (2000; 150 ± 10 pc), Knude & Hog (1998; 100 pc) and Wichmann et al. (1998a; 190 ± 27 pc), all also using *Hipparcos* data. Based on starlight polarization and CO observations, Rizzo, Morras, & Arnal (1998) estimate the distance at 130–170 pc. Knude & Nielsen (2001) find a distance to Lupus 2 of 360 pc. Franco (2002) finds evidence supporting $\sim$150 pc as a distance to Lupus 1. We settled on 150 pc as a weighted average to use here.

Most of the currently known members of this cluster have been discovered from extremely wide-field observations, e.g., the *ROSAT* All-Sky Survey. Assuming the cluster is at a distance of 150 pc, some of these surveys cover >50 pc. Tachihara et al. (2001) estimate $\sim 10^4\ M_\odot$ in gas and dust and a mean density of ~ 2 stars pc^{-3}. Isolated star formation appears to be ongoing here.

There are about 75 stars with rotational information, spectral types, and V and I magnitudes available. In the process of rederiving reddening, we found apparently negative reddening for five stars, for which we used a most likely reddening of $A_I = 0$. Because of a concerted effort by Wichmann and Krautter and collaborators, there are about 40 known P, and there are $v \sin i$ values for most of the stars with periods.

A7. η CHAMAELEONIS

This cluster is one of the closest open clusters to us, and new members are rapidly being discovered. It is currently estimated that there may be as many as 15–40 systems total within a 2° region (Lawson et al. 2002), suggesting a stellar density of ~ 1 or 2 stars pc^{-3}. We assumed a distance of 97 pc (Lawson et al. 2002).

There are only 12 stars with rotational information, spectral types, and V and I magnitudes currently available in the literature for this cluster. In the process of rederiving reddening, we found apparently negative reddening for one star, for which we used a most likely reddening of $A_I = 0$. Somewhat surprisingly, all of the rotational data available in the literature are periods. Like TW Hya,

because it is so close, this cluster provides the potential for nearby studies of disk evolution, so additional rotation data could prove useful for investigating the connection between disks and rotation rates.

A8. TW HYDRA

This cluster is possibly the nearest region of recent star formation, and new members are being discovered at a rapid pace. We assumed this cluster was at $\sim$60 pc and $\sim$10 Myr old (Song, Bessell, & Zuckerman 2002; Webb et al. 1999). This cluster is too close for Bertout et al. (1999) to find a distance, but they are able to conclude that the depth of the cluster is 20 pc, comparable to the angular size of the association.

There is little nebulosity left in this dispersed cluster, which is partly why it was only recently recognized as a cluster. Since the membership is most likely far from complete, stellar number density cannot be calculated for this cluster but seems to be $\lesssim$1 pc^{-3}.

There are 36 stars with rotational information, spectral types, and V and I magnitudes currently available in the literature for this cluster. In the process of rederiving reddening, we found apparently negative reddening for a handful of stars, for which we used a most likely reddening of $A_I = 0$. With the exception of one star (TW Hydra itself), only $v \sin i$ data are available for this cluster, and there are 19 stars available in the spectral type range K5–M2. Because this cluster is so close, it provides a laboratory for studies of disk evolution (e.g., Bary, Weintraub, & Kastner 2003), so it would be particularly useful to obtain additional studies of rotation rates in this cluster.

A9. IC 2391/2602

These two open clusters are nearly identical and are often grouped together for analysis, so we follow suit here. Pinsonneault et al. (1998) obtains 151–153 pc for both clusters, with very little reddening toward either cluster. van Leeuwen (1999) concludes that IC 2602 is at 155 pc, whereas IC 2391 is at 140 pc. Prosser (1998) also uses a distance of 155 pc. We assumed a distance of 155 pc for both clusters.

These clusters have stellar densities of a few pc^{-3}, with a total mass of a few hundred $M_\odot$. Precise values of these numbers await membership surveys.

There are about 50 stars with rotational information, spectral types, and V and I magnitudes currently available in the literature for this cluster. In the process of rederiving reddening, we find that all of the stars have physically reasonable values of reddening. Nearly all of the $\sim$20 stars with P also have $v \sin i$.

A10. α PERSEI

The distance to α Persei is often quoted as $\sim$170 pc. Prosser (1998) refers to 165 pc, and de Zeeuw et al. (1999) refer to a distance of 177 ± 4 pc; Stauffer et al. (1999) obtain 176 pc (with $A_I = 0.17$). Similarly, van Leeuwen (1999) concludes that the cluster is at 170 pc, but O'Dell et al. (1994) finds 182 pc. We used 175 pc as a final estimate.

This open cluster has a stellar density of a few pc^{-3}, with a total mass of $\lesssim$1000 $M_\odot$.

There are about 90 stars with rotational information, spectral types, and V and I magnitudes currently available in the literature for this cluster. In the process of rederiving reddening, we found that all of the stars have physically reasonable values of reddening. Because several groups have specifically studied rotation in this cluster, nearly all of the $\sim$40 stars with P also have $v \sin i$.

A11. PLEIADES

For the distance to this well-studied cluster, we assumed 132 pc. Prosser (1998) cites 127 pc (and $A_I = 0.10$). Pinsonneault et al. (1998) obtain $\sim$124 pc, van Leeuwen (1999) gets 125 pc, and O'Dell et al. (1994), 132 pc. This cluster is about 13 pc across, encompassing $\sim$1000 $M_\odot$ in stars; there are, on average, a few stars pc^{-3} at most.

There are about 140 stars with rotational information, spectral types, and V and I magnitudes currently available in the literature for this cluster. In the process of rederiving reddening, we found apparently negative reddening for only one star, for which we used a most likely reddening of $A_I = 0.07$. As in α Persei, because others have intensively sought rotation information in this cluster, nearly all of the $\sim$40 stars with P also have $v \sin i$.

REFERENCES

Alcalá, J., Krautter, J., Covino, E., Neuhaeuser, R., Schmitt, J. H. M. M., & Wichmann, R. 1997, A&A, 319, 184
Alcalá, J., Krautter, J., Schmitt, J. H. M. M., Covino, E., Wichmann, R., & Mundt, R. 1995, A&AS, 114, 109
Allen, L., Myers, P. C., Di Francesco, J., Mathieu, R., Chen, H., & Young, E. 2002, ApJ, 566, 993
Alves, J., Lada, C., & Lada, E. 2000, Ap&SS, 272, 213
Armitage, P., Clarke, C., & Palla, F. 2003, MNRAS, 342, 1139
Balachandran, S., Lambert, D. L., & Stauffer, J. R. 1988, ApJ, 333, 267
———. 1996, ApJ, 470, 1243
Barnes, J. R., Collier Cameron, A., James, D. J., & Steeghs, D. 2001, MNRAS, 326, 1057
Barnes, S. 2003, ApJ, 586, 464
Barnes, S., Sofia, S., Prosser, C. F., & Stauffer, J. R. 1999, ApJ, 516, 263
Barrado y Navascués, D., Stauffer, J. R., & Patten, B. M. 1999, ApJ, 522, L53
Bary, J., Weintraub, D., & Kastner, J. 2003, ApJ, 586, 1136
Basri, G., & Martin, E. 1999, ApJ, 510, 266
Batalha, C., Batalha, N. M., Alencar, S. H. P., Lopes, D. F., & Duarte, E. S. 2002, ApJ, 580, 343
Batalha, C. C., et al. 1998, A&AS, 128, 561
Bertout, C., Robichon, N., & Arenou, F. 1999, A&A, 352, 574
Bessell, M. S. 1991, AJ, 101, 662
Boesgaard, A. M., Armengaud, E., & King, J. R. 2003, ApJ, 582, 410
Bouvier, J. 1990, AJ, 99, 946
———. 1996, A&AS, 120, 127
Bouvier, J., & Appenzeller, I. 1992, A&AS, 92, 481
Bouvier, J., & Bertout, C. 1989a, A&A, 211, 99
———. 1989b, A&A, 218, 337
Bouvier, J., Bertout, C., Benz, W., & Mayor, M. 1986, A&A, 165, 110
Bouvier, J., Cabrit, S., Fernandez, M., Martin, E. L., & Matthews, J. M. 1993, A&A, 272, 176

Bouvier, J., Covino, E., Kovo, O., Martin, E. L., Matthews, J. M., Terranegra, L., & Beck, S. C. 1995, A&A, 299, 89
Bouvier, J., Forestini, M., & Allain, S. 1997a, A&A, 326, 1023
Bouvier, J., Stauffer, J. R., Martin, E. L., Barrado y Navascues, D., Wallace, B., & Bejar, V. J. S. 1998, A&A, 336, 490
Bouvier, J., et al. 1997b, A&A, 318, 495
———. 2003, A&A, in press (astro-ph/0306551)
Carpenter, J. M., Hillenbrand, L. A., & Skrutskie, M. F. 2001, AJ, 121, 3160
Carpenter, J. M., Hillenbrand, L. A., Skrutskie, M. F., & Meyer, M. 2002, AJ, 124, 1001
Chelli, A., Carrasco, L., Mújica, R., Recillas, E., & Bouvier, J. 1999, A&A, 345, L9
Chen, H., Grenfell, T. G., Myers, P. C., & Hughes, J. D. 1997, ApJ, 478, 295
Choi, P. I., & Herbst, W. 1996, AJ, 111, 283
Clarke, C., & Bouvier, J. 2000, MNRAS, 319, 457
Comerón, F., Neuhäuser, R., & Kass, A. A. 2000, A&A, 359, 269
Comerón, F., Rieke, G. H., & Neuhäuser, R. 1999, A&A, 343, 477
Covino, E., Alcala, J. M., Allain, S., Bouvier, J., Terranegra, L., & Krautter, J. 1997, A&A, 328, 187
Covino, E., Terranegra, L., Franchini, M., Chavarria-K, C., & Stalio, R. 1992, A&AS, 94, 273
Crawford, I. 2000, MNRAS, 317, 996
Cunha, L., Smith, V. V., & Lambert, D. L. 1998, ApJ, 493, 195
D'Antona, F., & Mazzitelli, I. 1994, ApJS, 90, 467 (DAM)
de Geus, E. J., de Zeeuw, P. T., & Lub, J. 1989, A&A, 216, 44
DeWarf, L. E., Sepinksy, J. F., Guinan, E. F., Ribas, I., & Nadalin, I. 2003, ApJ, 590, 357
de Zeeuw, P., Hoogerwerf, R., de Bruijne, J. H. J., Brown, A. G. A., & Blaauw, A. 1999, AJ, 117, 354
Doppman, G. W., Jaffe, D. T., & White, R. J. 2003, AJ, in press (astro-ph/0308522)
Dubath, P., Reipurth, B., & Mayor, M. 1996, A&A, 308, 107
Duncan, D. K. 1993, ApJ, 406, 172
Edwards, S., et al. 1993, AJ, 106, 372
Feigelson, E., Casanova, S., Montmerle, T., & Guibert, J. 1993, ApJ, 416, 623
Feigelson, E., & Kriss, G. 1981, ApJ, 248, L35
———. 1989, ApJ, 338, 262
Flaccomio, E., Micela, G., Sciortino, S., Favata, F., Corbally, C., & Tomaney, A. 1999, A&A, 345, 521
Franchini, M., Covino, E., Stalio, R., Terranegra, L., & Chavarria-K, C. 1992, A&A, 256, 525
Franchini, M., Magazzù, A., & Stalio, R. 1988, A&A, 189, 132
Franco, G. A. P. 2002, MNRAS, 331, 474
Gagné, M., & Caillault, J.-P. 1994, ApJ, 437, 361
Gagné, M., Caillault, J.-P., & Stauffer, J. 1995, ApJ, 445, 280
Gahm, G. F., Gullbring, E., Fischerstrom, C., Lindroos, K. P., & Loden, K. 1993, A&AS, 100, 371
Gameiro, J. F., & Lago, M. T. V. T. 1993, MNRAS, 265, 359
Gauvin, L., & Strom, K. 1992, ApJ, 385, 217
Genzel, R., Reid, J. J., Moran, J. M., & Downes, D. 1981, ApJ, 244, 884
Ghez, A. M., McCarthy, D. W., Patience, J. L., & Beck, T. L. 1997, ApJ, 481, 378
Granzer, T., Schüssler, M., Caligari, P., & Strassmeier, K. G. 2000, A&A, 355, 1087
Greene, T., & Lada, C. 1997, AJ, 114, 2157
———. 2000, AJ, 120, 430
———. 2002, AJ, 124, 2185
Greene, T., & Meyer, M. 1995, ApJ, 450, 233
Gregorio-Hetem, J., Lepine, J. R. D., Quast, G. R., Torres, C. A. O., & de La Reza, R. 1992, AJ, 103, 549
Gullbring, E., & Gahm, G. 1996, A&A, 308, 821
Haisch, K., Lada, E., & Lada, C. 2001, ApJ, 553, L153
Hamilton, C., Herbst, W., Mundt, R., Bailer-Jones, C. A. L., & Johns-Krull, C. M. 2003, ApJ, 591, L45
Hamilton, C., Herbst, W., Shih, C., & Ferro, A. J. 2001, ApJ, 554, L201
Hartigan, P. 1993, AJ, 105, 1511
Hartigan, P., Strom, K., & Strom, S. 1994, ApJ, 427, 961
Hartmann, L. 1998, ApJ, 495, 385
———. 2001, AJ, 121, 1030
———. 2002, ApJ, 566, L29
Hartmann, L., & Stauffer, J. 1989, AJ, 97, 873
Henize, K., & Mendoza, E. 1973, ApJ, 180, 115
Herbig, G. H., & Bell, K. R. 1988, Lick Obs. Bull., 1111
Herbst, W., Bailer-Jones, C. A. L., & Mundt, R. 2001, ApJ, 554, L197
Herbst, W., Bailer-Jones, C. A. L., Mundt, R., Meisenheimer, K., & Wackermann, R. 2002, A&A, 396, 513
Herbst, W., & Koret, D. 1988, AJ, 96, 1949
Herbst, W., Rhode, K. L., Hillenbrand, L. A., & Curran, G. 2000, AJ, 119, 261
Herbst, W., & Shevchenko, V. 1999, AJ, 118, 1043
Hillenbrand, L. A. 1997, AJ, 113, 1733
Hillenbrand, L. A., & Hartmann, L. W. 1998, ApJ, 492, 540
Hillenbrand, L. A., Meyer, M., & Carpenter, J. 2004, in preparation
Hillenbrand, L. A., Strom, S. E., Calvet, N., Merrill, K. M., Gatley, I., Makidon, R. B., Meyer, M. R., & Skrutskie, M. F. 1998, AJ, 116, 1816
Huenemoerder, D. P., Lawson, W. A., & Feigelson, E. D. 1994, MNRAS, 271, 967
Hughes, J., & Hartigan, P. 1992, AJ, 104, 680
Hughes, J., Hartigan, P., & Clampitt, L. 1993, AJ, 105, 571
Hughes, J., Hartigan, P., Krautter, J., & Kelemen, J. 1994, AJ, 108, 1071
James, D., Jardine, M. M., Jeffries, R. D., Randich, S., Collier Cameron, A., & Ferreira, M. 2000, MNRAS, 318, 1217
Jayawardhana, R., Monhanty, S., & Basri, G. 2002, ApJ, 578, L141
Joergens, V., & Guenther, E. 2001, A&A, 379, L9
Joergens, V., Guenther, E., Neuhäuser, R., Fernández, M., & Vijapurkar, J. 2001, A&A, 373, 966
Kastner, J. H., Huenemoerder, D. P., Schulz, N. S., Canizares, C. R., & Weintraub, D. A. 2002, ApJ, 567, 434
Kearns, K., & Herbst, W. 1998, AJ, 116, 261
Kenyon, S., Dobrzycka, D., & Hartmann, L. 1994, AJ, 108, 1872
Kenyon, S., & Gomez, M. 2001, AJ, 121, 2673
Kenyon, S., & Hartmann, L. 1995, ApJS, 101, 117
King, J., Krishnamurthi, A., & Pinsonneault, M. H. 2000a, AJ, 119, 859
King, J., Soderblom, D. R., Fischer, D., & Jones, B. F. 2000b, ApJ, 533, 944
Knude, J., & Hog, E. 1998, A&A, 338, 897
Knude, J., & Nielsen, A. S. 2001, A&A, 373, 714
Königl, A. 1991, ApJ, 370, L39
Königl, A., & Pudritz, R. 2000, in Protostars and Planets IV, ed. V. Mannings, A. P. Boss, & S. S. Russell (Tucson: Univ. Arizona Press), 759
Krautter, J., Wichmann, R., Schmitt, J. H. M. M., Alcala, J. M., Neuhauser, R., & Terranegra, L. 1997, A&AS, 123, 329
Lamm, M., Mundt, R., Bailer-Jones, C. A. L., & Herbst, W. 2002, BAAS, 34, 758
Lawson, W. A., Crause, L. A., Mamajek, E. E., & Feigelson, E. D. 2001, MNRAS, 321, 57
———. 2002, MNRAS, 329, L29
Lawson, W. A., Feigelson, E. D., & Huenemoerder, D. P. 1996, MNRAS, 280, 1071
Leggett, S. K. 1992, ApJS, 82, 351
Leggett, S. K., Allard, F., & Hauschildt, P. H. 1998, ApJ, 509, 836
Luhman, K. L., & Rieke, G. 1999, ApJ, 525, 440
Luhman, K. L., Rieke, G., Young, E. T., Cotera, A. S., Chen, H., Rieke, M. J., Schneider, G., & Thompson, R. I. 2000, ApJ, 540, 1016
Lyo, A.-R., Lawson, W. A., Mamajek, E. E., Feigelson, E. D., Sung, E.-C., & Crause, L. A. 2003, MNRAS, 338, 616
Magazzù, A., Rebolo, R., & Pavlenko, Y. 1992, ApJ, 392, 159
Makidon, R., et al. 2004, AJ, in press
Mamajek, E. E., Lawson, W. A., & Feigelson, E. D. 1999, ApJ, 516, L77
———. 2000, ApJ, 544, 356
Marino, A., et al. 2003, A&A, 407, 63
Martin, E., Montmerle, T., Gregorio-Hetem, J., & Casanova, S. 1998, MNRAS, 300, 733
Mathieu, R. D. 2003, in IAU Symp. 215, ed A. Maeder & P. Eenens, in press (astro-ph/0303199)
McNamara, B. 1990, ApJ, 350, 348
Messina, S. 2001, A&A, 371, 1024
Messina, S., Rodonò, M., & Guinan, E. F. 2001, A&A, 366, 215
Mizuno, A., et al. 1999, PASJ, 51, 859
Montes, D., & Ramsey, L. W. 1999, in ASP Conf. Ser. 158, Solar and Stellar Activity: Similarities and Differences, ed. C. J. Butler & J. G. Doyle (San Francisco: ASP), 302
Montmerle, T., Grosso, N., Tsuboi, Y., & Koyama, K. 2000, ApJ, 532, 1097
Muzerolle, J., Hillenbrand, L., Calvet, N., Briceno, C., & Hartmann, L. 2003, ApJ, 592, 266
Neuhäuser, R., Brandner, W., Alves, J., Joergens, V., & Comerón, F. 2002, A&A, 384, 999
Neuhäuser, R., & Comerón, F. 1999, A&A, 350, 612
Neuhäuser, R., Sterzik, M. F., Schmitt, J. H. M. M., Wichmann, R., & Krautter, J. 1995, A&A, 297, 391
Neuhäuser, R., et al. 1998, A&A, 334, 873
O'Dell, M., & Collier Cameron, A. 1993, MNRAS, 262, 521
O'Dell, M. A., Hendry, M. A., & Collier Cameron, A. 1994, MNRAS, 268, 181
O'Dell, M. A., Hilditch, R. W., Collier Cameron, A., & Bell, S. A. 1997, MNRAS, 284, 874
Padgett, D. 1996, ApJ, 471, 847
Park, B., Sung, H., Bessell, M., & Kang, Y. 2000, AJ, 120, 894
Patience, J., Ghez, A. M., Reid, I. N., & Matthews, K. 2002, AJ, 123, 1570

Patten, B., & Simon, T. 1996, ApJS, 106, 489
Petr, M., Fernandez, M., Alcala, J. M., & Covino, E. 1999, in Star Formation 1999, ed. T. Nakamoto (Nobeyama: Nobeyama Radio Obs.), 403
Pinsonneault, M., Stauffer, J., Soderblom, D. R., King, J. R., & Hanson, R. B. 1998, ApJ, 504, 170
Pizzolato, N., Maggio, A., Micela, G., Sciortino, S., & Ventura, P. 2003, A&A, 397, 147
Preibisch, T., & Smith, M. D. 1997, A&A, 322, 825
Prosser, C. F. 1998, The Open Cluster Database (Tucson: NOAO)
Prusti, T., Whittet, D. C. B., & Wesselius, P. R. 1992, MNRAS, 254, 361
Randich, S., Aharpour, N., Pallavicini, R., Prosser, C. F., & Stauffer, J. R. 1997, A&A, 323, 86
Randich, S., Martin, E. L., Lopez, R. J. G., & Pallavicini, R. 1998, A&A, 333, 591
Randich, S., Pallavicini, R., Meola, G., Stauffer, J. R., & Balachandran, S. C. 2001, A&A, 372, 862
Randich, S., Schmitt, J. H. M. M., & Prosser, C. 1996, A&A, 305, 785
Rebull, L. M. 2001, AJ, 121, 1676
Rebull, L. M., Hillenbrand, L. A., Strom, S. E., Duncan, D. K., Patten, B. M., Pavlovsky, C., Makidon, R., & Adams, M. 2000, AJ, 119, 3026
Rebull, L. M., Wolff, S. C., Strom, S. E., & Makidon, R. B. 2002a, AJ, 124, 546 (RWSM02)
Rebull, L. M., et al. 2002b, AJ, 123, 1528
Reid, N. 2003, MNRAS, 342, 837
Rhode, K. L., Herbst, W., & Mathieu, R. D. 2001, AJ, 122, 3258
Rizzo, J. R., Morras, R., & Arnal, E. M. 1998, MNRAS, 300, 497
Rydgren, A. E., Zak, D. S., Vrba, F. J., Chugainov, P. F., & Zajtseva, G. V. 1984, AJ, 89, 1015
Schwartz, R. D. 1977, ApJS, 35, 161
Shevchenko, V. S., & Herbst, W. 1998, AJ, 116, 1419
Shu, F., Najita, J., Shang, H., & Li, Z.-Y. 2000, in Protostars and Planets IV, ed. V. Mannings, A. P. Boss & S. S. Russell (Tucson: Univ. Arizona Press), 789
Smith, M. A., Beckers, J. M., & Barden, S. C. 1983, ApJ, 271, 237
Soderblom, D., King, J. R., Siess, L., Jones, B. F., & Fischer, D. 1999, AJ, 118, 1301
Soderblom, D., Stauffer, J. R., MacGregor, K. B., & Jones, B. F. 1993, ApJ, 409, 624
Song, I., Bessell, M. S., & Zuckerman, B. 2002, A&A, 385, 862
Stahler, S. W. 1983, ApJ, 274, 822
Stassun, K. G., Mathieu, R. D., Mazeh, T., & Vrba, F. J. 1999, AJ, 117, 2941
Stauffer, J., Hartmann, L. W., Burnham, J. N., & Jones, B. F. 1985, ApJ, 289, 247
Stauffer, J., Hartmann, L. W., & Jones, B. F. 1989, ApJ, 346, 160
Stauffer, J., Hartmann, L. W., Prosser, C. F., Randich, S., Balachandran, S., Patten, B. M., Simon, T., & Giampapa, M. 1997, ApJ, 479, 776
Stauffer, J., et al. 1999, ApJ, 527, 219
Sterzik, M., Alcalá, J. M., Covino, E., & Petr, M. G. 1999, A&A, 346, L41
Strom, K. M., Strom, S. E., Edwards, S., Cabrit, S., & Skrutskie, M. F. 1989, AJ, 97, 1451
Strom, K. M., Strom, S. E., & Merrill, K. M. 1993, ApJ, 412, 233
Sung, H., Bessell, M. S., & Lee, S.-W. 1997, AJ, 114, 2644
Swenson, F. J., Faulkner, J., Rogers, F. J., & Iglesias, C. A. 1994, ApJ, 425, 286
Tachihara, K., Dobashi, K., Mizuno, A., Ogawa, H., & Fukui, Y. 1996, PASJ, 48, 489
Tachihara, K., Toyoda, S., Onishi, T., Mizuno, A., Fukui, Y., & Neuhäuser, R. 2001, PASJ, 53, 1081
Terndrup, D., Krishnamurthi, A., Pinsonneault, M. H., & Stauffer, J. R. 1999, AJ, 118, 1814
Terndrup, D., Stauffer, J. R., Pinsonneault, M. H., Sills, A., Yuan, Y., Jones, B. F., Fischer, D., & Krishnamurthi, A. 2000, AJ, 119, 1303
Tinker, J., Pinsonneault, M., & Terndrup, D. 2002, ApJ, 564, 877
Torres, G., Guenther, E. W., Marschall, L. A., Neuhäuser, R., Latham, D. W., & Stefanik, R. P. 2003, AJ, 125, 825
Torres, G., Neuhäuser, R., & Latham, D. W. 2001, in ASP Conf. Ser. 244, Young Stars Near Earth: Progress and Prospects, eds. R. Jayawardhana & T. Greene (San Francisco: ASP), 283
Tschape, R., & Rudiger, G. 2001, A&A, 377, 84
van Leeuwen, F. 1999, A&A, 341, L71
Vogel, S. N., & Kuhi, L. V. 1981, ApJ, 245, 960
Vrba, F., Chugainov, P. F., Weaver, W. B., & Stauffer, J. S. 1993, AJ, 106, 1608
Walker, M. F. 1969, ApJ, 155, 447
———. 1983, ApJ, 271, 642
———. 1990, PASP, 102, 726
Walter, F. 1992, AJ, 104, 758
Walter, F., Brown, A., Mathieu, R. D., Myers, P. C., & Vrba, F. J. 1988, AJ, 96, 297
Walter, F., Vrba, F. J., Mathieu, R. D., Brown, A., & Myers, P. C. 1994, AJ, 107, 692
Warren, W. H., & Hesser, J. E. 1978, ApJS, 36, 497
Webb, R. A., Zuckerman, B., Platais, I., Patience, J., White, R. J., Schwartz, M. J., & McCarthy, C. 1999, ApJ, 512, L63
White, R., & Basri, G. 2003, ApJ, 582, 1109
Whittet, D. C. B., Kirrane, T. M., Kilkenny, D., Oates, A. P., Watson, F. G., & King, D. J. 1987, MNRAS, 224, 497
Whittet, D. C. B., Prusti, T., Franco, G. A. P., Gerakines, P. A., Kilkenny, D., Larson, K. A., & Wesselius, P. R. 1997, A&A, 327, 1194
Wichmann, R., Bastian, U., Krautter, J., Jankovics, I., & Rucinski, S. M. 1998a, MNRAS, 301, L39 Q1
Wichmann, R., Bouvier, J., Allain, S., & Krautter, J. 1998b, A&A, 330, 521
Wichmann, R., Covino, E., Alcalá, J. M., Krautter, J., Allain, S., & Hauschildt, P. H. 1999, MNRAS, 307, 909
Wichmann, R., Krautter, J., Covino, E., Alcala, J. M., Neuhaeuser, R., & Schmitt, J. H. M. M. 1997, A&A, 320, 185
Wichmann, R., et al. 2000, A&A, 359, 181
Wilking, B., Bontemps, S., Schuler, R. E., Greene, T. P., & André, P. 2001, ApJ, 551, 357
Wolff, S., Strom, S., & Hillenbrand, L. 2004, ApJ, in press
Zuckerman, B., Webb, R. A., Schwartz, M., & Becklin, E. E. 2001, ApJ, 549, L233